

# We are IntechOpen, the world's leading publisher of Open Access books Built by scientists, for scientists

4,800

Open access books available

122,000

International authors and editors

135M

Downloads

Our authors are among the

154

Countries delivered to

TOP 1%

most cited scientists

12.2%

Contributors from top 500 universities



WEB OF SCIENCE™

Selection of our books indexed in the Book Citation Index  
in Web of Science™ Core Collection (BKCI)

Interested in publishing with us?  
Contact [book.department@intechopen.com](mailto:book.department@intechopen.com)

Numbers displayed above are based on latest data collected.  
For more information visit [www.intechopen.com](http://www.intechopen.com)



# Porous Apatite Coating on Various Titanium Metallic Materials via Low Temperature Processing

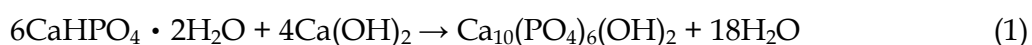
Takamasa Onoki

*Department of Materials Science, Graduate School of Engineering,  
Osaka Prefecture University  
Japan*

## 1. Introduction

Nowadays, hydroxyapatite (HA) is widely used as bioceramics in reconstructive surgery, in dentistry and as drug delivery materials due to the good biocompatibility and osteoconductivity [Hench, 1998]. One of the limitations for the usage of these materials is their low mechanical strength. Thus, many researchers focus on the development of new biomaterials, that combine the osteoconductive characteristics of bioactive ceramics with sufficient strength and toughness for load-bearing applications. The combination of high strength of the metals with osteoconductive properties of bioactive ceramics makes HA coated metallic implants, which titanium (Ti) or its alloys was mainly used, very attractive for the load-bearing applications in orthopedic and dental surgery [Long & Rack, 1998]. A plasma spraying method has been conventionally employed for the HA coating. However, this method has some problems (e.g. a poor coating-substrate adherence, lack of HA crystallinity) for the long-term performance and lifetime of the implants [Aoki, 1994]. Therefore, new HA coating methods have attracted great interests in recent years for replacing the high temperature techniques like plasma spraying.

Hydrothermal hot-pressing (HHP) method is a possible processing route for producing a ceramic body at relatively low temperatures (under 300°C) [Yamasaki et al., 1986]. The compression of samples under hydrothermal conditions accelerates densification of inorganic materials. It is known that the water of crystallization in calcium hydrogen phosphate dihydrate ( $\text{CaHPO}_4 \cdot 2\text{H}_2\text{O}$ ; DCPD) is slowly lost below 100°C [Peelen et al., 1991]. If the released water can be utilized as a reaction solvent during the HHP treatment, it is to be expected that the joining HA to metal can be achieved simultaneously under the hydrothermal condition, in addition to the synthesis and solidification of HA through the chemical reaction as follows [Hosoi et al., 1996]:



In our previous reports, we have proposed a HHP method for bonding HA ceramics and pure Ti, Ti alloys, Magnesium alloy, and Ti based bulk metallic glass by hydrothermal hot-pressing techniques [Onoki et al., 2003a, 2003b, 2005, 2006, 2008a, 2008b, 2009a, 2009b, 2010a, 2010b, 2010c, 2011].

Ti-based alloys are beneficial for biomedical applications due to their low density, excellent biocompatibility, and corrosion resistance. Combining the advantages of both bulk metallic glass and Ti-based alloy, Ti-based bulk metallic glasses are expected to be applied as a new type of biomaterial. However, it is well-known that the surface of bulk metallic glasses, which are bioinert, must be bioactive to use as bone replacing medical/dental materials as well as Ti and its alloys. Recently, it was reported a concept called "Growing Integrated Layer" [GIL] that improves adhesion performance without cracking and peeling the ceramic coatings [6]. In particular, if the metallic glass or alloy contains a very reactive component like Ti, it can grow on the bulk metallic materials with its "root" in the bulk. This was named the "Growing Integrated Layer" or "Graded Intermediate Layer [GIL]" and the "Growing Integration Process [GIP]" for its formation process. Multiple layered, laminated, integrated, graded, and diffused coatings have been investigated to decrease the stress accumulation, which however, it is not easy, particularly when the interface is sharp. Even widely diffused interface(s) of larger micron sizes are preferable for joining and coating bulk ceramics on metallic materials. Such a GIL of oxide films grown from the "seed," i.e., the most reactive component in the bulk metallic materials is interesting as a novel process of oxide film formations, especially because the oxide film can be fabricated in a solution at such low temperatures as RT-200°C when chemical and/or electrochemical potentials are added. Thermal stress accumulation can be avoided in those low temperature formations of the ceramic film on the metal.

In this chapter, some hydrothermal technologies as low temperature process were described as HA ceramics bonding/coating methods and surface modification of various Ti metallic materials, especially pure Ti and Ti-based bulk metallic glass.

## 2. Bonding HA ceramics and pure Ti

### 2.1 Hydrothermal hot-pressing

In this study, DCPD used as a starting powder was prepared by mixing 1.0M calcium nitrate solution (99.0%;  $\text{Ca}(\text{NO}_3)_2 \cdot 4\text{H}_2\text{O}$ , KANTO CHEMICAL CO., INC., Japan) and 1.0M diammonium hydrogen phosphate solution (98.5%;  $(\text{NH}_4)_2\text{HPO}_4$ , KANTO CHEMICAL CO., INC., Japan). The mixing was carried out at a room temperature (approximately 20°C). In order to control the pH value of the mixing solution, acetic acid (99.5%; KANTO CHEMICAL CO., INC., Japan) and ammonia solution (28.0-30.0%; KANTO CHEMICAL CO., INC., Japan) were added. The value of pH was kept around 8.5 initially, and then changed to 6.0 using the acetic acid and ammonia solution after the mixing in order to prevent the formation of impurities and to produce pure DCPD powders. It has been shown from preliminary tests that when no control of the pH was conducted the synthesized DCPD contained the impurities such as  $\text{CaHPO}_4$  (DCPA), and amorphous calcium phosphate (ACP). The precipitate from the mixture was filtered and washed with deionized water and acetone. The washed filter cake was oven-dried at 50°C for 24 hours, and then the dried cake was ground to a powder. No impurity in the synthesized DCPD used was detected by powder X-ray diffraction. The synthetic DCPD and calcium hydroxide (95.0%;  $\text{Ca}(\text{OH})_2$ ; KANTO CHEMICAL CO., INC., Japan) were mixed in a mortar for 60min with a Ca/P ratio of 1.67 which was stoichiometric ratio of HA.

A commercially available pure Ti rod (Nilaco, Japan, diameter: 20mm, thickness: 10mm, purity: 99.5% JIS Grade1), 20mm in diameter, was used in this experiment. The Ti rod was cut into disks with a thickness of 10mm. The disks were cleaned in deionized water and

acetone by using an ultrasonic cleaner. The Ti surfaces were finished using 1500# emery paper. After the surface finish with emery paper, the titanium disks were washed again by deionized water, and then dried in air. The powder mixture and Ti disks were placed into the middle of the autoclave simultaneously, as shown in Fig.1.

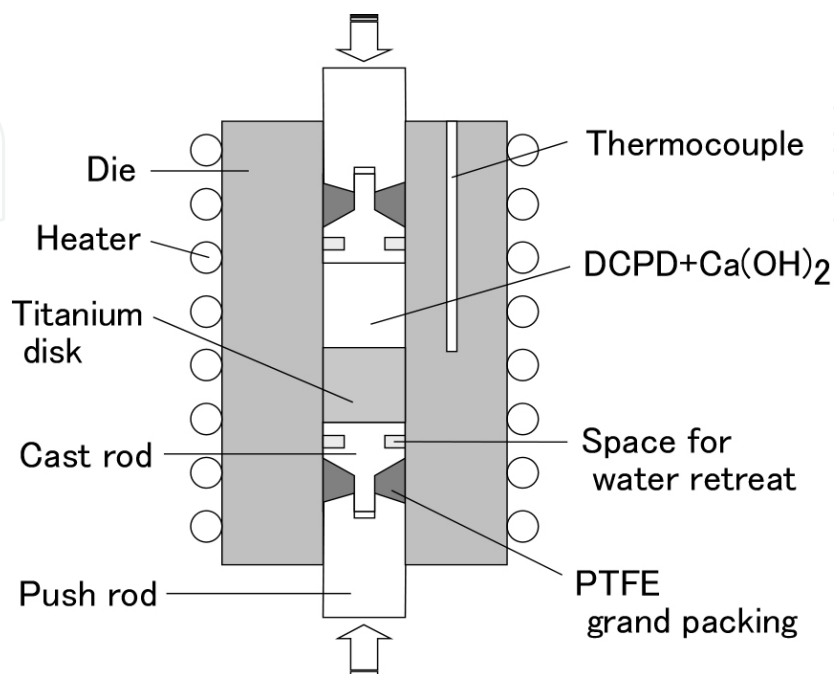


Fig. 1. Schematic illustration of the autoclave for Hydrothermal Hot-Pressing(HHP).

The autoclave made of steel has a pistons-cylinder structure with an inside diameter of 20 mm. The pistons possess escape space for hydrothermal solution squeezed from the sample, and this space regulates the appropriate hydrothermal conditions in the sample. A grand packing of polytetrafluoroethylene (PTFE) is placed between a cast rod and push rod. The PTFE was used to prevent leakage of the hydrothermal solutions. The stainless steel (SUS304) autoclave has pistons within a cylindrical structure with an inside diameter of 20 mm. The pistons enable the hydrothermal solution squeezed from the sample to escape, and this regulates the appropriate hydrothermal conditions in the sample. Polytetrafluoroethylene (PTFE) is packed between a cast rod and a push rod. The PTFE was used to prevent leakage of the hydrothermal solutions. Pressure of 40 MPa was initially applied to the sample through the push rods from the top and bottom at room temperature. After initial loading the autoclave was heated to 150°C at 10°C/min with a sheath-type heater, and then the temperature was kept constant for two hours. The axial pressure was kept at 40 MPa during the hydrothermal hot-pressing treatment. After the HHP treatment, the autoclave was naturally cooled to room temperature, and the sample was removed from the autoclave.

## 2.2 Adhesion properties evaluation

3-point bending tests were conducted to obtain an estimate of the fracture toughness for the HA/Ti interface as well as for the HA ceramics made by the HHP method. Core-based specimens were used for the fracture toughness tests following the ISRM suggested method[Hashida, 1993]. The configuration of the core-based specimen is schematically

shown in Fig.2. In order to measure the interface toughness, stainless steel-rods were glued to the HA/Ti body and solidified HA body using epoxy resin in order to prepare standard core specimens specified in the ISRM suggested method. A pre-crack was introduced in the HA/Ti interface, as shown in Fig.2. The depth and width of the pre-crack were 5mm and 50 $\mu$ m, respectively. In order to determine the fracture toughness of the HA only, HA specimens were sandwiched and glued with stainless steel rods. In this type specimens, a pre-crack was introduced in the center of HA ceramics. The specimens were loaded at a cross-head speed of 1mm/min until a fast fracture took place. The stress intensity factor  $K$  was employed to obtain an estimate of the fracture property of the HA/Ti interface and the HA ceramics, using the following equation:

$$K = 0.25(S / D) \cdot Y'_c \cdot (F / D^{1.5}) \quad (2)$$

where  $D$  is diameter of the specimen (20mm),  $S(=3.33D)$  is supporting span,  $F$  is load,  $Y'_c$  is the dimensionless stress intensity factor. The value of  $Y'_c$  can be found in the literature reference [Hashida, 1993].  $Y'_c$  was fixed 7.0 due to the initial crack depth, as shown in Fig.2. The critical stress intensity  $K_c$  was computed from peak load at the onset of fast fracture. It should be mentioned here that the formula given in Eq.(2) is derived under the assumption of isotropic and homogeneous materials. The HA/Ti bonded specimen used in this study consists of 2 or 3 kinds of the materials. While exact anisotropic solution is needed for the quantitative evaluation of the stress intensity factor, the isotropic solution in Eq.(2) is used to obtain an estimate of the fracture toughness for the HA and HA/Ti specimens.

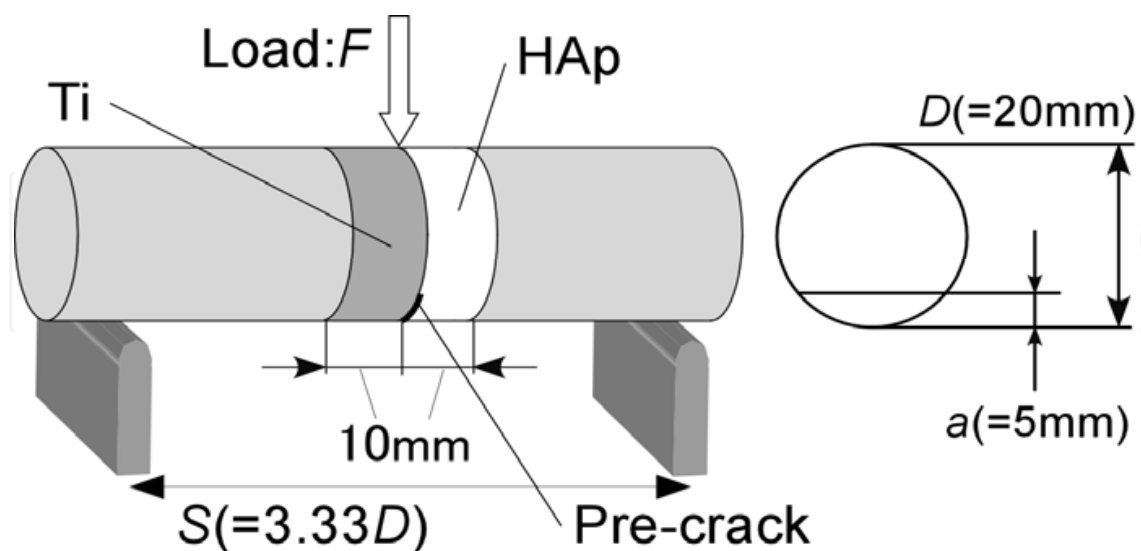


Fig. 2. Schematic illustration of 3-point bending test.

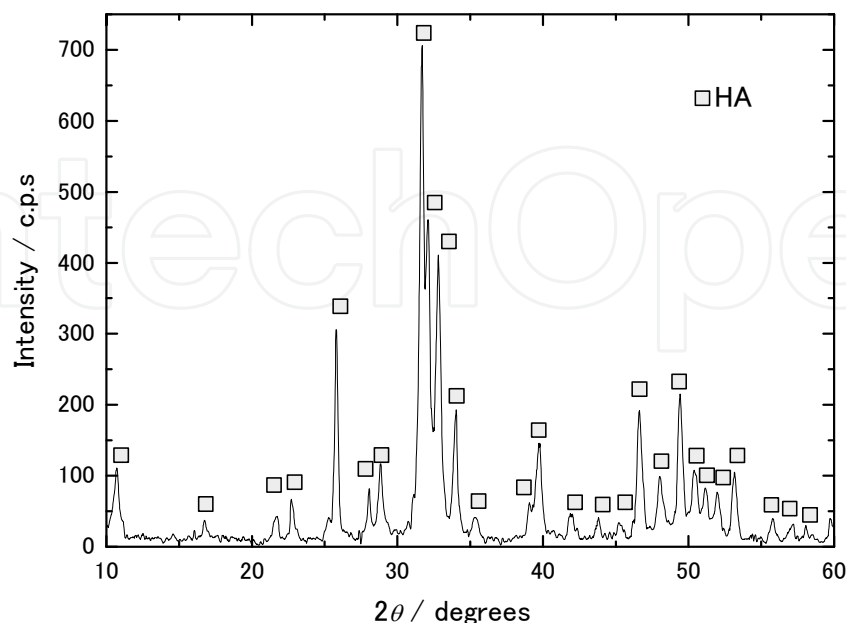


Fig. 3. X-ray diffraction pattern of the HA ceramics.

### 2.3 HA/Ti Bonding and its adhesive properties

It is seen that the shrinkage started at approximately 90°C. This temperature is close to the dehydration temperature of DCPD. Thus, it is thought that the shrinkage is initiated by the dehydration of DCPD. The shrinkage rate became larger with the increasing temperature, and then the shrinkage rate became smaller. The shrinkage continued during the HHP treatment. The pressure was held at 40MPa constant for the whole period of HHP treatment. As given in Fig.3, X-ray diffraction analysis showed that the DCPD and  $\text{Ca}(\text{OH})_2$  powder materials were completely transformed into HA by the HHP treatment. As demonstrated in Fig.4, the HA ceramics could be bonded to the Ti disks at the low temperature of 150°C using the above-mentioned HHP treatment. The density of the HA ceramics prepared by the HHP in this study was 1.9 g/cm<sup>3</sup>. In addition to the DCPD powder, three different types of powders were used as a starting material: HA and  $\beta$ -tri calcium phosphate ( $\beta$ -TCP). No bonding with a Ti disk was observed, when the above starting powders were used and treated by the HHP under the conditions of 150°C and 40MPa. Thus, DCPD was the only starting material that produced HA/Ti bonded bodies among the precursors for HA used in this study.

Fig.5 shows a photograph of the fracture surface in the bonded HA/Ti body after 3-point bending test. It can be noted that the crack initiated from the pre-crack tip and propagated not along the HA/Ti interface, but into the HA. This observation suggests that the fracture toughness of the HA/Ti interface is close to or higher than that of the HA ceramics only. The critical stress intensity factor  $K_c$  was 0.30 MPam<sup>1/2</sup> for the HA ceramics, and 0.25 MPam<sup>1/2</sup> for the bonded HA/Ti. The toughness data are the average value obtained from at least five specimens. The  $K_c$  value for the bonded HA/Ti body gives a slightly lower value than that of the HA ceramics only. The difference in  $K_c$  data is potentially due to the residual stress



induced by the thermal expansion mismatch between HA and Ti. The  $K_c$  value achieved for the pure Ti was close to the highest value obtained for the Ti alloys in our research [Onoki et al. 2003]. The fracture appearance in Fig.5 may suggest that the interface toughness should be equal or higher than that of the HA ceramics only. While further development is needed to improve the fracture property of the solidified HA, the HHP treatment may have the advantage over the plasma-spraying technique in the preparation of thermodynamically stable HA without decomposition. The above results demonstrate the usefulness of the HHP method for bonding HA and Ti in order to produce a bioactive layer in biomaterials.

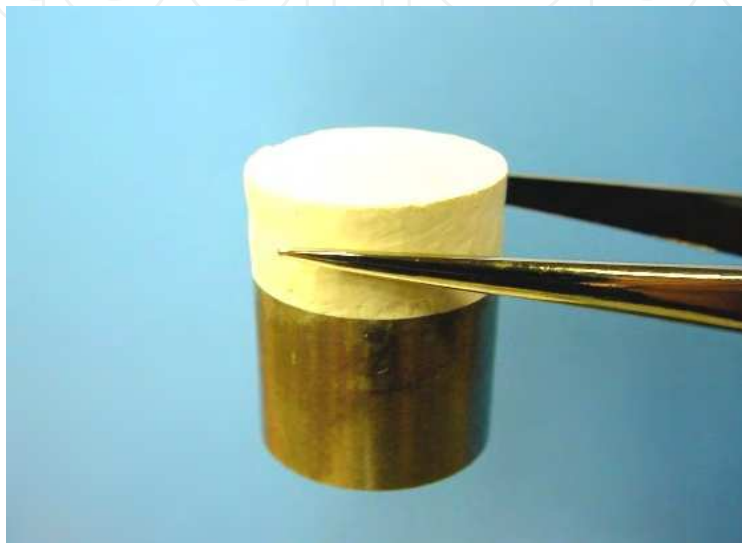


Fig. 4. Photograph of the bonded body of HA ceramics and Ti metal (20mm in diameter).

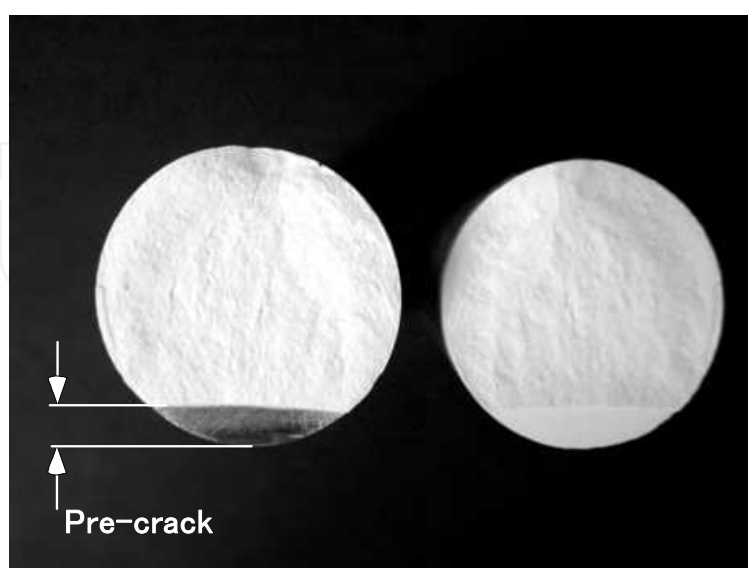


Fig. 5. Photograph of the fracture surface in a HA/Ti specimen after 3point bending test. Note that the crack propagated into HA.

## 2.4 Ti surface analysis by X-ray photoelectron spectroscopy (XPS)

Traditionally, Ti and its alloys have been reported to be bioinert. When embedded in the human body, a fibrous tissue encapsulates the implant isolating it from the surrounding bone forms. Since conventional metals as biomaterials are usually covered with metal oxides, surface oxide films on metals play an important role not only against corrosion but also regarding tissue compatibility. The composition of surface oxide film varies according to environmental changes, although the film is macroscopically stable. Passive surfaces co-exist in close contact with electrolytes, undergoing a continuous process of partial dissolution and re-precipitation from the microscopic viewpoint [Kelly, 1982]. In this sense, the surface composition constantly changes according to the environment. The film on titanium consists of amorphous or low-crystalline and non-stoichiometric  $\text{TiO}_2$  [Kelly, 1982]. The surface oxide film of titanium just after polishing in water contains not only  $\text{Ti}^{4+}$  but also  $\text{Ti}^{3+}$  and  $\text{Ti}^{2+}$  [Beck, 1973; Kelly, 1982]. Hydrated phosphate ions are adsorbed by a hydrated titanium oxide surface during the release of protons [Hanawa, 1992]. Calcium ions are adsorbed by phosphate ions adsorbing on a titanium surface, and, eventually, calcium phosphate is formed. The above mentioned phenomena are characteristic in titanium and titanium alloys [Hanawa, 1992]. In this regard, an anatase-like structure is effective for apatite nucleation [Wei et al., 2002ab], whereas the naturally formed oxide film on titanium surface is mainly amorphous. The ability of titanium in order to form calcium phosphate on itself is one of the reasons for its better hard-tissue compatibility than those of other metals. This property is applied to the surface modification of titanium and its alloys to improve hard-tissue compatibility. In the case of alkali-heat-treated titanium, calcium and phosphate are orderly deposited, and calcium deposition is the pre-requisite for phosphate deposition [Yang et al., 1999].

It is easily expected that the bonding properties of the HA/Ti interface prepared by the HHP method can be depended on the Ti surface conditions. As preliminary experimental results, Ti surface finished in wet environment can be achieved bonding to HA ceramics through the above mentioned HHP method. However, Ti surfaces before the HHP processing have not been investigated precisely. The present study aims to investigate Ti surface properties through X-ray photoelectron spectroscopy (XPS) analysis. Particular attention was been paid to chemical composition and oxidation states of Ti in surface films in order to explain the bonding mechanism of Ti and HA ceramics by the HHP.

A commercially available pure Ti rod was used. The Ti surfaces were finished using 1500# emery paper in *air* and *water* conditions. After the emery paper finish, the Ti disks were cleaned in deionized water and ethanol by using an ultrasonic cleaner, and then dried in air. XPS was performed with an electron spectrometer (ULVAC-PHI, ESCA1600). All binding energies given in this paper are relative to the Fermi level, and all spectra were excited with the monochromatized Al  $K\alpha$  line (1486.61 eV). The spectrometer was calibrated against Au  $4f_{7/2}$  (binding energy, 84.07 eV) and Au  $4f_{5/2}$  (87.74 eV) of pure gold and Cu  $2p_{3/2}$  (932.53 eV), Cu  $2p_{1/2}$  (952.35 eV), and Cu Auger  $L_{3M_{4,5}M_{4,5}}$  line (kinetic energy, 918.65 eV) of pure copper. The energy values were based on published data [Asami & Hashimoto, 1977]. The reproducibility of the results was confirmed several times under the same conditions.

In order to clarify the surface related chemical characteristics of the Ti, XPS analysis was performed for the specimens as-polished mechanically in *air* or *water* environments. The XPS spectra of the specimens over a wide binding energy region exhibited peaks of Ti 2p, O



1s and C 1s. The C1s spectrum showing a peak at around 285.0 eV arose from a contaminant hydrocarbon layer covering the topmost surface of the specimens. The spectra of the O 1s electron energy regions about *air* and *water* finishing are obtained. In particular, the O 1s spectrum was composed of at least two overlapping peaks which were so-called OM and OH oxygen in water finishing Ti specimens. The OM oxygen corresponds to  $O^{2-}$  ion in oxyhydroxide and/or oxide, and the OH oxygen is oxygen linked to protons in the surface film, being composed of OH ions and bound water in the surface films. As shown in Fig.6(a) and (b), The deconvoluted XPS spectra of the O 1s region contained three peaks originating from oxide ( $O^{2-}$ ), hydroxide or hydroxyl groups ( $OH^-$ ), and hydrate and/or adsorbed water ( $H_2O$ ) [Beck,1973; Kelly, 1982]. Calculated fitting curves area of the samples finished in *air* and *water* environment was summarized in table.1. From these results, hydroxide or hydroxyl groups ( $OH^-$ ) of the water finishing sample increased compared with the air finishing sample. There is no distinguished difference between *air* and *water* finishing specimens within the Ti 2p spectra.

XPS characterization revealed differences in the Ti surfaces properties between water and air in finishing circumstances before the HHP treatment, as shown in Fig. 6(a) and (b). Compared with the air finishing Ti samples, the O 1s region XPS spectra of the water finishing Ti samples was significantly assigned hydroxide or hydroxyl groups ( $OH^-$ ) and hydrate and/or adsorbed water ( $H_2O$ ). The HA/Ti bonding via the HHP processing could be achieved in only water finished Ti samples, as shown in Fig.4. On the other hand, the Ti samples finishing in air circumstance could not achieved the bonding to the HA ceramics. From these results, the bonding model between Ti and HA ceramics through the HHP method is suggested and summarized in below.

Calcium, phosphate and hydorate ions within the HHP autoclave solution are adsorbed on a titanium surface, and eventually calcium phosphate is formed, and then solidified as hydroxyapatite ceramics, as shown in Fig. 4. Similar model has been reported by Kokubo *et al* during apatite derived from Simulated Body Fluid (SBF) [Kokubo & Takadama, 2006]. It was guessed that the HA/Ti bonding behavior depended on amount of hydroxide or hydroxyl groups ( $OH^-$ ) and hydrate and/or adsorbed water ( $H_2O$ ). In order to bond Ti and HA ceramics through the HHP techniques, it is important factors that hydroxide or hydroxyl groups ( $OH^-$ ) and hydrate and/or adsorbed water ( $H_2O$ ) are remained on Ti surfaces. There is a threshold of amount of hydroxide or hydroxyl groups ( $OH^-$ ) between air and water finished surfaces.

	$O^{2-}$	$OH^-$	$H_2O$
(a) Air	62.50%	18.20%	19.30%
(b) Water	58.20%	24.60%	17.20%

Table 1. Calculated fitting curve area portion of O1s XPS spectra shown in Fig.6(a) and (b).

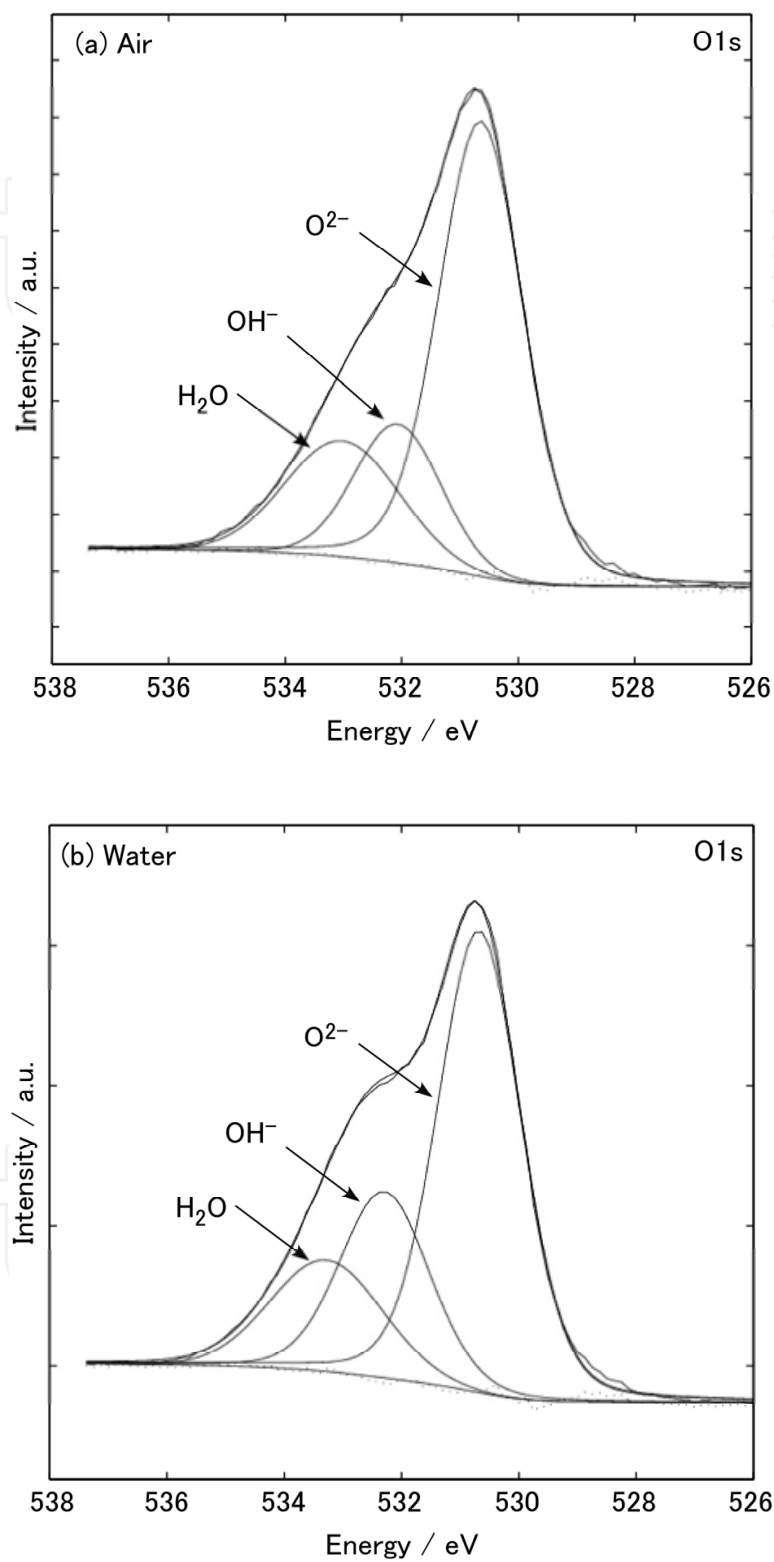


Fig. 6. O 1s XPS spectra of Ti surfaces finished in air (a) and water (b) environments (after curve fitting analysis).

### 3. Surface modification of metallic materials

#### 3.1 Pure Ti

Recently, it was reported a concept called “Growing Integrated Layer” [GIL] that improves adhesion performance without cracking and peeling the ceramic coatings. Formation of a bioactive titanium dioxide ( $\text{TiO}_2$ ) hydro-gel layer has been shown to improve the nucleation of calcium phosphate during chemical deposition. The  $\text{TiO}_2$  layer could be prepared by alkaline [Wei et al., 2002ab; Kim et al., 2000; Wen et al., 1998ab],  $\text{H}_2\text{O}_2$  [Ostuki et al., 1997; Kaneko et al., 2001; Rohanizadeh et al., 2004], sol-gel [Oswald et al., 1999] or heat treatment methods [Rohanizadeh et al., 2004]. It is demonstrated that the treatment of Ti with a NaOH solution followed by heat treatment at 873 K forms a crystalline phase of sodium titanate layer on the Ti surface resulting in improved adhesion of apatite coating prepared by incubation in simulated body fluid (SBF) [Wei et al., 2002ab; Kim et al., 2000; Takadama et al., 2001]. The authors concluded that release of the sodium ions from the sodium titanate layer causes formation of Ti-OH groups that react with the calcium ions from the SBF and form calcium titanate, which then could act as nucleation sites for apatite crystal formation [Takadama et al., 2001]. Alkali treatment results in the formation of a  $\text{TiO}_2$  layer leading to a negatively charged surface, which in turn attracts cations such as calcium ions [Wen et al., 1998a]. Etching with acid followed by alkali treatment was also investigated to combine the surface roughness increase due to acid treatment and formation of a  $\text{TiO}_2$  bioactive layer [Wei et al., 1998b].  $\text{TiO}_2$  could be also prepared using  $\text{H}_2\text{O}_2$  alone or a mixture of acid/ $\text{H}_2\text{O}_2$  or metal chlorides/ $\text{H}_2\text{O}_2$  solutions [[Ostuki et al., 1997; Kaneko et al., 2001; Rohanizadeh et al., 2004]. Thus, it is expected that the interface strength of HA/Ti bonded bodies prepared by the HHP method can be improved, if the above-mentioned bioactive layer can be formed on the Ti surface. The present study examines the effects of various surface modification of Ti with 5M NaOH solution on the HA/Ti bonding behavior via the HHP method.

A commercially available pure Ti rod (99.5%; Nilaco, Japan), 20mm in diameter, was used. The Ti rod was cut into disks with a thickness of 10mm. And the disks were cleaned in deionized water and acetone by using an ultrasonic cleaner. The Ti surfaces were finished using 1500# emery paper. The Ti surface without a special surface modification is referred to as “NORMAL” surface. After the emery paper finish, the titanium disks were washed by deionized water, and then dried in air. In order to form bioactive  $\text{TiO}_2$  and sodium titanate layer on the Ti surface, some of the “NORMAL” disks were treated with alkali solution (5M NaOH) under the same conditions used in the literatures [Wei et al., 2002ab; Kim et al., 2000; Takadama et al., 2001]. The Ti disks were immersed in the NaOH solution for 24 hours. Some of the Ti disks were further heat-treated at 873 K for 1 hour after the NaOH immersion for 24 hours. It has been reported that the reaction layer formed by the NaOH immersion at 333 K for 24 hours was easily detached by adhesive tape [Kim et al., 1997]. In order to avoid the detachment of the reaction layer, the Ti needed to be heated up to 873 K for 1 hour in an air. The Ti disk with the heat treatment at 873 K is labeled as “HEAT” surface, and without the heat treatment is labeled as “IMMER” surface. In our previous study [Onoki et al., 2003], the surface modification of Ti alloys (Ti-15Mo-5Zr-3Al and Ti-6Al-2Nb-1Ta) with NaOH solution (5M NaOH) at 323 K for 2 hours could significantly improve the bonding strength of the HA/Ti. Thus, it is expected that the same surface treatment on the Ti surface may enhance the bonding strength of the HA/Ti. Some of the “NORMAL” Ti disks were placed into a small vessel with the NaOH solution and heated up to 323 K for 2

hours. Ti disk treated with the hydrothermal NaOH solution is referred to as “HYDRO” surface. After the above-mentioned treatments with NaOH solution, the Ti disks were washed by deionized water, and then dried in air. The surface conditions of Ti disks are summarized in Table 2.

In order to characterize the Ti surfaces, the surfaces were observed using scanning electron microscopy (SEM: HITACHI FE-SEM S-4300, Japan) and were examined using FT-Raman spectroscopy. The microprobe instrument used for the FT-Raman spectroscopy consisted of a spectrometer (JOBIN YVON-HORIBA SPEX) fitted with a microscope (OLYMPUS-BX30, Japan) which had spatial resolution on the sample close to 1μm. The 632.8nm line of an He-Ne laser was used as excitation, focused in a spot of approximately 1μm diameter, with an incident power of 2mW.

Type	NaOH Treatment		873K Heat
	Temp.(K)	Time(h)	
NORMAL	-	-	-
IMMER	333	24	-
HEAT	333	24	1h
HYDRO	423	2	-

Table 2. Conditions of the surface modifications of the Ti disks.

In order to characterize the reaction products formed on the Ti surface products, observation by SEM of the Ti surfaces treated with the NaOH solution were conducted for the “NORMAL”, “IMMER”, “HEAT” and “HYDRO” specimens, respectively. Furthermore, analytical results of Raman spectroscopy analysis were obtained of the “NORMAL”, “IMMER”, “HEAT” and “HYDRO” specimens, respectively.

The surface morphology of the “NORMAL” specimen exhibits finishing lines in the nearly horizontal direction, which were formed at the stage of surface polishing with the emery paper. Raman spectra for the “NORMAL” specimen shows no distinct peak. The surface morphology of the “IMMER” specimen has a very fine network structure (0.1μm scale) with finishing lines in the perpendicular direction. In the Raman spectra of the “IMMER” specimen, the peaks of TiO<sub>2</sub> (both of anatase and rutile phase) and sodium titanate (Na<sub>2</sub>Ti<sub>5</sub>O<sub>11</sub>) could be detected. The surface morphology of the “HEAT” specimen has a sponge-like structure and no finishing lines are visible on it. In the Raman spectra of the “HEAT” specimen, the peaks of TiO<sub>2</sub> (only rutile phase) and sodium titanate (Na<sub>2</sub>Ti<sub>5</sub>O<sub>11</sub>) could be detected. Indeed, it has been reported in the literature [Kim et al., 1997] that in a Ti specimen treated with NaOH solution dehydration of the reaction layer took place by the

post heating at 873 K and that the anatase phase as observed in the “IMMER” specimen was changed into rutile phase entirely.

The surface morphology of the “HYDRO” specimen has a needle like structure, as shown in Fig.7. In the Raman spectra of the “HYDRO” specimen, the peaks of  $\text{TiO}_2$  (both of anatase and rutile phase) and sodium titanate ( $\text{Na}_2\text{Ti}_5\text{O}_{11}$ ) could be detected as shown in Fig.7. As reported in the literature [Kim et al., 1997], we have also observed that the reaction layer of the “IMMER” specimen was easily peeled off by adhesive tape, and that the post heating at 873 K was necessary in order to prevent the delamination of the reaction layer from the Ti specimen. However, it was shown that in the “HYDRO” specimen no delamination of the reaction layer took place in peeling tests with adhesive tape, without post heating process. It is shown from the Raman spectra that the reaction layers formed on the Ti surface are essentially composed of the identical chemical compounds both for the “IMMER” and “HYDRO” specimens.

### 3.2 HA bonding behavior

For all the Ti surface modifications, the HA ceramics was successfully bonded to the Ti using the HHP method. The NaOH treatments on Ti surface were useful in obtaining HA/Ti bonding body regardless of the any NaOH treatment conditions (see Table3). The fracture toughness for the HA/Ti specimens was obtained from 3-point bending tests. The fracture toughness data are given in Table 3 along with the reaction products characterized by the Raman spectra. The fracture toughness data are the average value obtained from at least five specimens. The fracture toughness,  $K_c$  for the “IMMER” and “HEAT” specimens shows a slightly lower value than that of the “NORMAL” specimens. The fracture toughness data of the “HYDRO” specimens is higher than that of “NORMAL” specimens. In the literature [Kim et al., 1997], SBF soaking tests were conducted on “IMMER” Ti specimen and “HEAT” Ti specimen at 310 K. The growth rate of bone-like apatite on the Ti surface was shown to be larger for the “IMMER” specimen than that in the “HEAT” specimen. Based on the above observation, it has been concluded that the formation of anatase in the reaction layer produced by the treatment with 5M NaOH solution accelerates the growth rate of bone-like apatite in the Ti surface. On the other hand, it was shown that the reaction layer of “IMMER” specimen had poor adhesion with Ti substrates in contrast with “HEAT” specimen. The lower fracture toughness in the “IMMER” specimen may be due to the poor adhesion property, in spite of the formation of anatase in the reaction layer. The plausible cause for the lower fracture toughness in the “HEAT” specimen may be attributed to the lack of anatase, even though the adhesion property was improved significantly through the post heat treatment. As described above, no delamination of the reaction layer occurred for the “HYDRO” specimen in the tests conducted using adhesive tape. The higher adhesion property in conjunction with the formation of anatase may provide the explanation for the larger fracture toughness value in the “HYDRO” specimen.

It was revealed that the hydrothermal surface modification with the NaOH solution was the most effective technique among the surface treatment methods used in this study in the improvement of the bonding strength of the HA/Ti interface produced by the HHP method. The fracture toughness for the “HYDRO” specimen showed 40% increase with respect to that of the “NORMAL” specimen.



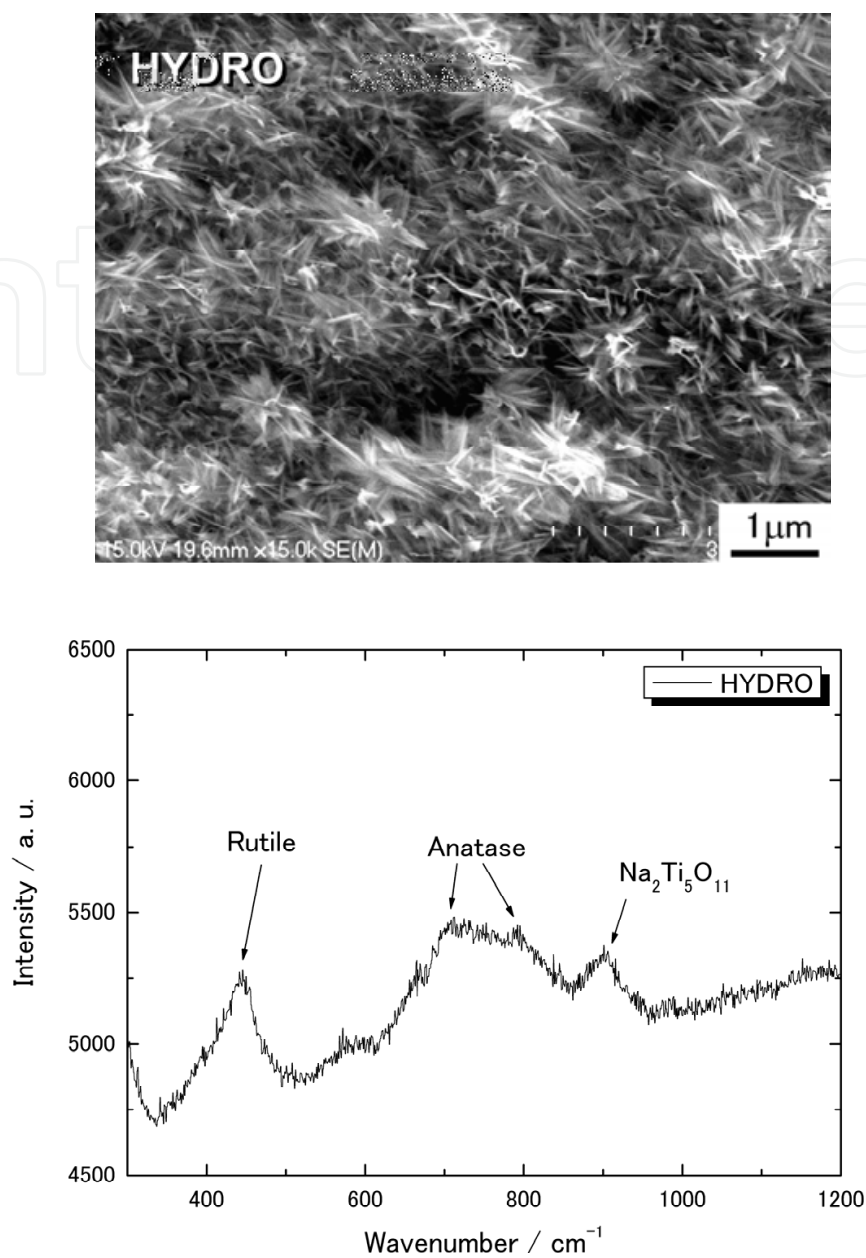


Fig. 7. SEM Micrograph and FT-Raman Spectra of the “HYDRO” Ti surface.

Type	Titanium Oxide		Sodium Titanate	$K_C$ (MPam <sup>1/2</sup> )
	Anatase	Rutile		
NORMAL	–	–	–	0.25
IMMER	○	○	○	0.22
HEAT	–	○	○	0.21
HYDRO	○	○	○	0.35

Table 3. Characterization of the Ti surface products and the interface fracture toughness.



### 3.3 Ti based Bulk metallic glass

Bulk glassy alloys are promising materials for structural and functional uses due to their superior properties compared to their crystalline counterparts [Greer, 1995; Inoue, 2000; Ashby & Greer, 2006]. These alloys are known to exhibit high hardness, high tensile strength, and good fracture toughness. The unique properties of bulk glassy alloys make them extremely attractive for biomedical applications. The mechanical deformation behavior of biological materials, which is characterized by a high recovery of strain (above 2%) after deformation, is very different from that of common metallic materials [Li et al., 2000]. Another problem concerning metallic implants in orthopedic surgery is the mismatch of Young's modulus between a human bone and metallic implants. The bone is insufficiently loaded due to a mismatch called stress-shielding. From the viewpoint of the requirements toward implant materials for hard tissue replacement, a biomaterial with low elastic modulus is required. Glassy alloys have lower Young's modulus and an extremely high elastic limit of 2%. Since bulk glassy alloys have a unique ability to flex elastically with the natural bending of bone, they distribute stresses more uniformly. Faster healing rates will result from reduced stress shielding effects while minimizing stress concentrators.

Ingots of Ti-based bulk metallic glass ( $\text{Ti}_{40}\text{Zr}_{10}\text{Cu}_{36}\text{Pd}_{14}$ : BMG) were prepared by arc-melting the pure elements with purities above 99.9% in an argon atmosphere [Zhu et al., 2007]. Cylindrical rods (5mm diameter) were prepared by copper mold casting method. And cut into disks with a thickness in 2 mm. The BMG surfaces were finished using emery paper. After the surface finish with the emery paper, the BMG disks were degreased prior to hydrothermal-electrochemical experiment. After sonicated in acetone and rinsed with distilled water, disks were dried at ambient temperature. Glassy structure of the BMG was examined by X-ray diffraction patterns (XRD).

Recently, it was reported a concept called "Growing Integrated Layer" [GIL] that improves adhesion performance without cracking and peeling the ceramic coatings. In order to produce GIL on surface of the BMG, hydrothermal-electrochemical treatment was conducted, as shown in Fig.8 [Yoshimura et al., 2008]. The BMG substrate was used as the working anode and platinum substrate was used as the cathode. The distance between electrodes was kept at 4 cm. The active anodic surface area immersed in electrolyte was  $0.707 \text{ cm}^2$ . GIL was fabricated by the hydrothermal-electrochemical treatment at  $90^\circ\text{C}$  for 120 minutes in aqueous solutions of 5M NaOH as an electrolyte. A constant electric current of  $0.5 \text{ mA/cm}^2$  was applied between electrodes. After hydrothermal-electrochemical treatments, the specimens were removed from the electrolyte, washed with distilled water and then dried at  $80^\circ\text{C}$  for 2 hours in air. The GIL produced by the hydrothermal-Electrochemical method was observed by an scanning electron microscopy (SEM: Hitachi S-4500, Japan) in surface morphology and a cross section view. Surface products were removed from the BMG and observed by a transmission electron microscopy (TEM: Hitachi H-9000, Japan).

The BMG disks were examined by powder X-ray diffractions patterns. Broadened XRD patterns denote a glassy nature. For  $\text{Ti}_{40}\text{Zr}_{10}\text{Cu}_{36}\text{Pd}_{14}$ , a glassy state was confirmed as well as the literature [Zhu et al., 2007]. Surface morphology and cross section view of the GIL by the SEM observation were displayed in Fig.9 (a) and (b), respectively. The surfaces after the hydrothermal-electrochemical treatments had nanometer-scale meshed structure. The mesh products might be consisted of amorphous nano-rods from the results of SEM observations as shown in Fig.9. The nano-rods had amorphous structure and no crystalline phases like as

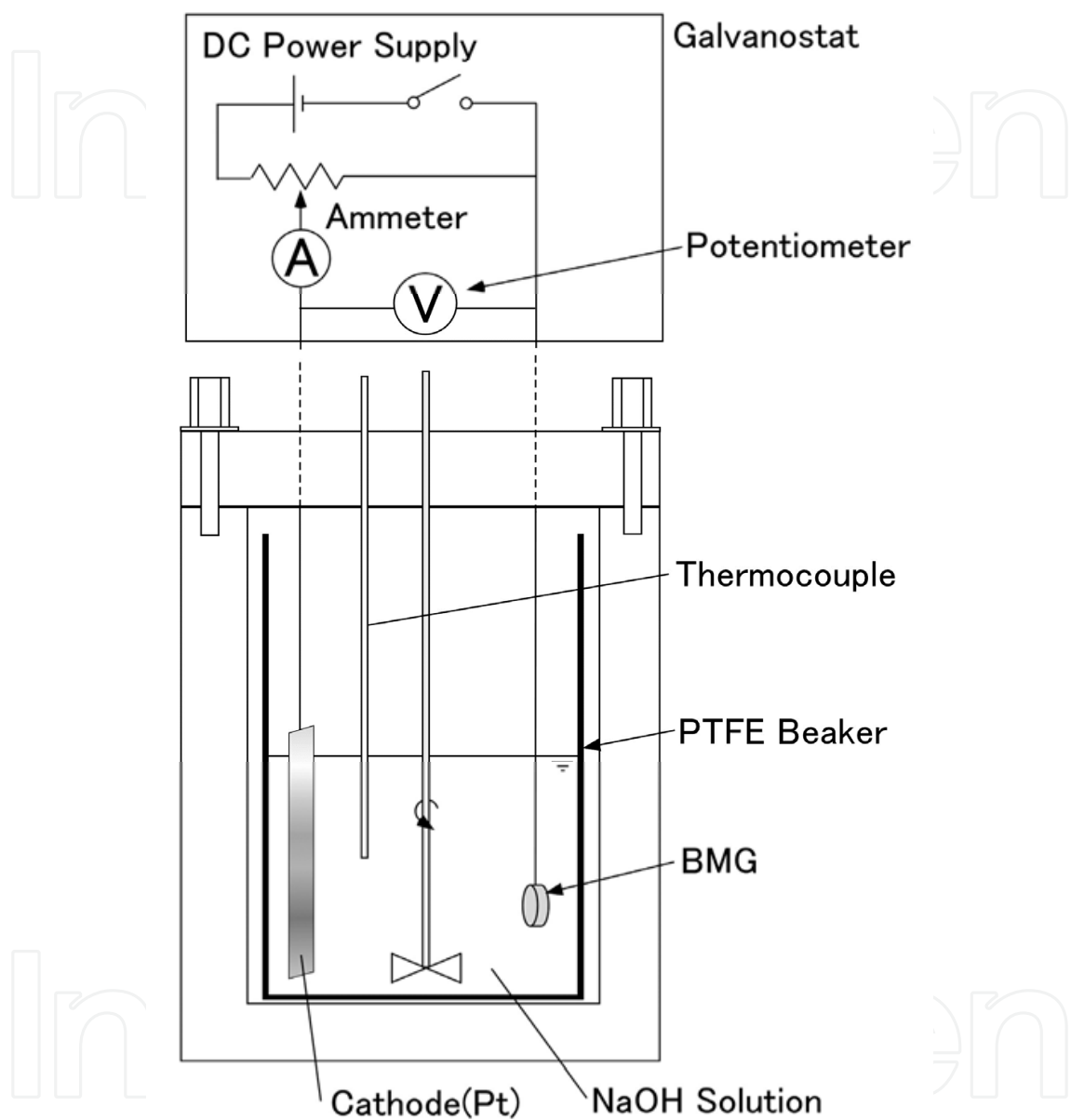


Fig. 8. Schematic illustration of experimental equipment for hydrothermal-electrochemical treatment.

titanate nanotubes [Onoki et al., 2009a]. Thin Film mode XRD analysis supported that the surface products formed on the BMG had the amorphous phase. Depth of the nano-meshed structure was approximately 1 $\mu$ m. It was supposed that the GIL was constructed between the BMG substrate and the nano-mesh materials.

Bonding hydroxyapatite ceramics and the BMGs could be achieved through the HHP treatment, like as shown in Fig.10. Because the BMG is essentially bioinert, the BMG without surface treatments has no HA bulk ceramics adhesion. It is easily guessed that the HA adhesive ability of the BMG surfaces is derived from the GIL made by the hydrothermal-electrochemical treatment. The bonding body was shaped in 5mm diameter structure like as Fig.4 by using grinder. In case of the BMG without the GIL, the bonding sample was easily separated into the HA ceramics and the BMG. However, the HA/BMG bonding body with the GIL was keep adhesive during the 5mm grinding process. The interface between the BMG and HA ceramics might have sufficient mechanical strength.

Since glass transition and crystallization onset temperatures of about  $\text{Ti}_{40}\text{Zr}_{10}\text{Cu}_{36}\text{Pd}_{14}$  have been reported at 396 and 445°C, respectively [Zhu et al., 2007], the uniquely mechanical properties of the bulk metallic glasses must be lost in case of adding over 400°C heat treatment. Lower temperature techniques (under 400°C) are required for surface bioactivity treatments for retaining the uniquely mechanical properties of the bulk metallic glasses. The operating temperature (maximum 150°C) of the above hydrothermal treatments are low enough. A series of hydrothermal techniques is expected to be one of the most useful methods for creating bioactivity to Ti-based bulk metallic glasses surfaces. Moreover, hydrothermal techniques are appropriate for compositing bulk metallic glassy materials and ceramics to provide complementary functions with other materials due to the low temperature of hydrothermal processing. By using other hydrothermal techniques [Onoki et al., 2006], HA ceramics coating on Ti-based BMG could be achieved.

As shown in Figs. 10(a) and (b), we observed near the interface between the HA and the BMGs with the hydrothermal-electrochemical treatments for 40 and 120 minutes, respectively. Amorphous nano-meshed structure on the BMG surface was disappeared during the hydrothermal hot-pressing (HHP) process for bonding HA ceramics and the BMGs. If HA precipitates into the nano-meshed structure, the nano structure can be watched in these SEM micrographs. However, there was no fragmented or remained nano-mesh. It is known that the surface amorphous products processed by low temperature solution are meta-stable phase and easily dehydrated and hydrolyzed [Kim et al., 1997; Onoki et al., 2008]. Consequently, it is guessed the amorphous products were consumed or decomposed during the HHP treatments. An intermediate layer between HA ceramics and the BMG was revealed in the SEM micrographs as shown in Figs. 10(a) and (b). It is observed that the greater hydrothermal-electrochemical treatment time, the thicker the intermediate layer became. Compared with Fig.9 and 10, the thickness of the GIL and the intermediate layer were estimated in almost same value, respectively. It was concluded that the intermediate layer was the GIL remained on the BMG. The intermediate layer would play a role of relaxation of thermal expansion misfit and bonding layer between the BMG and the HA ceramics. The BMG with the hydrothermal-electrochemical treatments for 10 minutes could not achieved the bonding the BMG and HA ceramics through the HHP. The 10minutes treated BMG had insufficient thickness of the intermediate layer. It is speculated that sufficient thickness of GIL is the most important factor for the bonding BMG and HA ceramics by the HHP method. From above shown Results and discussion, it is demonstrated that the hydrothermal techniques (hydrothermal-electrochemical treatment and hydrothermal hot-pressing) are necessary and useful for bonding between BMG and HA ceramics.

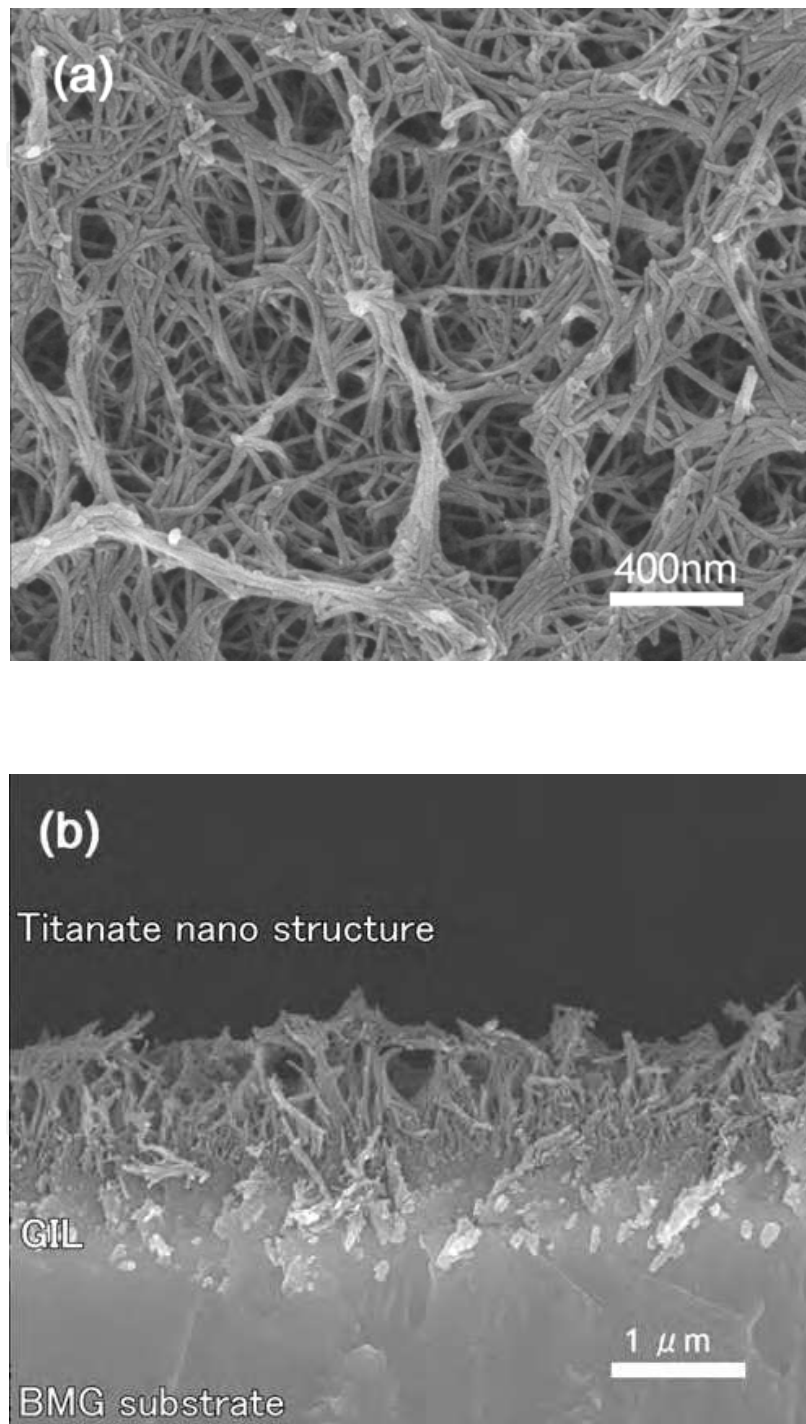


Fig. 9. SEM micrograph of BMG surface through hydrothermal-electrochemical treatment for 120 minutes (a) and in a cross sectional view(b), respectively.

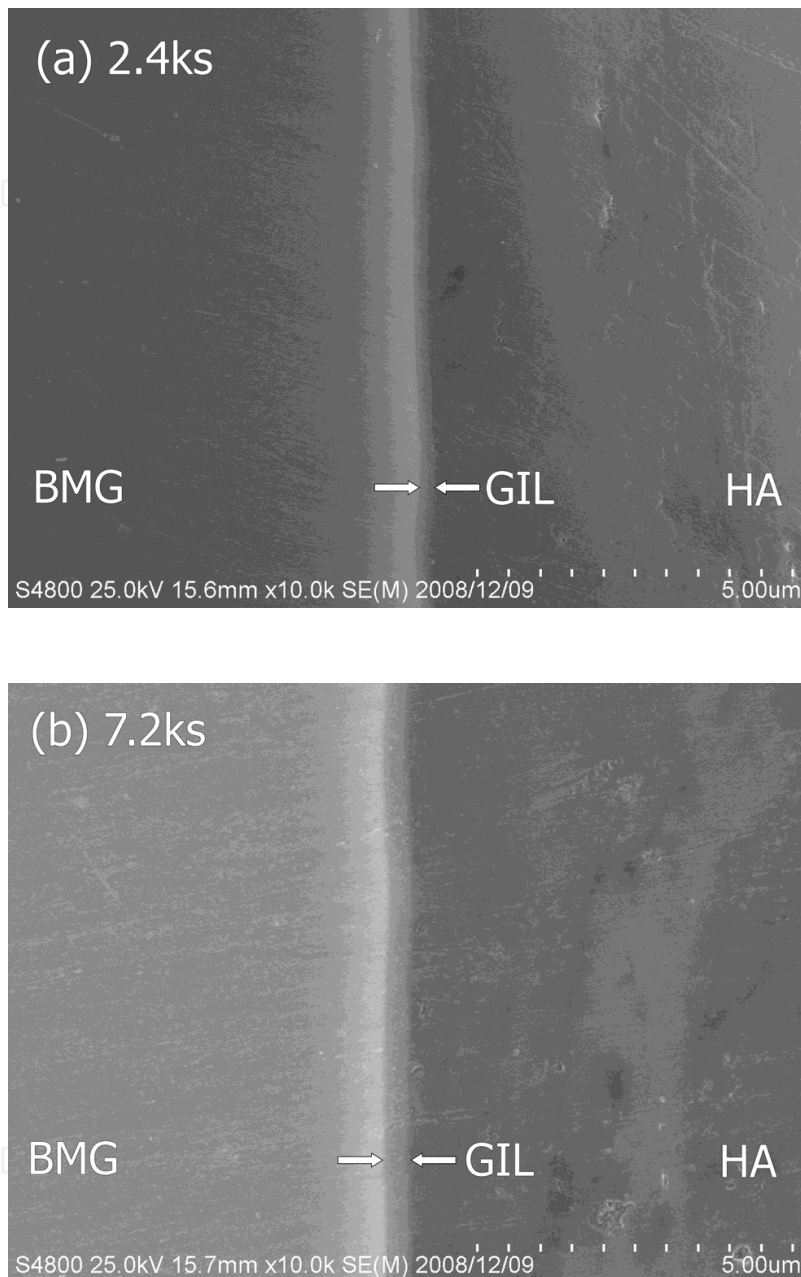


Fig. 10. SEM micrograph of the interface between HA ceramics and BMG disk with hydrothermal-electrochemical treatments for 40 (a) and 120 minutes(b), respectively.

#### 4. HA coating by Double layered capsule hydrothermal hot-pressing

##### 4.1 Introduction and using materials

In previous sections, it has been proposed a HHP method for bonding HA ceramics and pure Ti, Ti alloys and Ti based BMG by hydrothermal hot-pressing. HA ceramics was



bonded to the *flat* surface of a Ti disk using the HHP method at 150°C and 40MPa. The thickness of the HA ceramics bonded was about 10mm. It has been shown from three point bending tests that the fracture strength of the HA/Ti interface was equal to or higher than that of the HA ceramics. Additionally, X-ray diffraction analyses revealed that the HA ceramics bonded had high crystallinity without any decomposition and impurity. However, the HA bonding was achieved only on *flat* surfaces of Ti because of uniaxial pressing. In order for the hydrothermal method to be applicable to orthopedic and dental implant materials, we should develop a method for coating thin HA layer onto curved surface. This section describes a new methods for coating HA ceramics layer on Ti rod at the low temperature as low as 135°C by using the newly developed double layered capsule hydrothermal hot-pressing (DC-HHP) method, which utilizes isostatic pressing under hydrothermal conditions.

The synthetic DCPD and calcium hydroxide (95.0%;  $\text{Ca(OH)}_2$ ; KANTO CHEMICAL CO., INC., Japan) were mixed in a mortar for 60min with a Ca/P ratio of 1.67 which was stoichiometric ratio of HA. A commercially available pure Ti rod (99.5%; Nilaco, Japan), 1.5mm in diameter, was used in this study. The Ti rod was cut into a length of approximately 20mm. Ti surfaces were finished using #1500 emery paper. The rods were cleaned in deionized water and acetone by using an ultrasonic cleaner.

Recently, it has been reported that surface modifications for forming bonelike apatite can induce the high bioactivity of bioinert materials in simulated body fluid (SBF) [Kokubo et al., 2004]. In our previous research [Onoki et al., 2003], bonding HA ceramics and Ti alloys (Ti-15Mo-5Zr-3Al and Ti-6Al-2Nb-1Ta) was achieved by the HHP method through the surface modification of Ti alloys with alkali solution (5M NaOH). It is reported that the surface treatment of the Ti alloys with the alkali solution was very effective to improve the fracture strength of the interface between HA and Ti alloys produced by the HHP method. Based on the above results, the Ti rods used in this study were treated with 5M NaOH solution after the emery paper finish. The hydrothermal treatment with the NaOH solution was conducted at 150°C for 2 hours using a small vessel (volume: 7.5ml). After the surface treatment, the Ti rods were washed by deionized water, and then dried in air.

#### 4.2 Double layered capsule hydrothermal hot-pressing (DC-HHP) method

A new technique was developed in this study in order to prepare HA coating layers on a cylindrical rod with the objective of applying the hydrothermal hot-pressing method to a substrates with more complicated configurations, as shown in Fig.11. The newly developed method uses a cylindrical capsule having the double layered structure, which is subjected to isostatic pressing under hydrothermal conditions. A schematic illustration of the capsule in a cross section view is shown in Fig.12.

Firstly, the Ti rod and the powder mixture of DCPD and  $\text{Ca(OH)}_2$  were placed into a tube made of polyfluoroethylene (FEP). The weight of the powder mixture put into was approximate 0.1g. The initial diameter and thickness of the FEP tube was 1.8mm and 100 $\mu\text{m}$ . The FEP shrinks thermally by approximately 25% at around 130°C. The powder mixture was loaded into the FEP tube such that the Ti rod was concentrically positioned with respect to the tube axis. Both the ends of the FEP tube were fastened with paper staples. The sample assemblage encapsulated using the FEP tube is called “capsule I” in this study. Secondly, the capsule I was further encapsulated using a poly-vinylidene-chloride (PVC; 11 $\mu\text{m}$  thickness, Asahi-KASEI, Japan) film. Between the capsule I and PVC film, alumina powder



(3.0  $\mu\text{m}$  diameter; Buehler Ltd., USA) was placed. The thickness of the alumina powder layer was approximately 3mm. The capsule prepared using the PVC film is called “capsule II”. Then, the PVC film was sealed off using a thermo-compression method. As expected, the sealing of the capsule II was found to be crucially important for the subsequent hydrothermal treatment. No solidification and bonding of the HA ceramic layer was observed when there was a pre-existing defect in the thermally bonded PVC film and the water used for pressure application seeped into the capsule. Thus, the double layered capsule was vacuumed prior to sealing the capsule II, and left for 1 hour at the laboratory in order to check the seal tightness. Initially, a semi-permeable membrane for water was used instead of the FEP tube. However, it was observed that the fastened ends of the FEP tube could act as a narrow water flow-path. Thus, the thermally shrinkable FEP tube was used for capsule I in this study. The excessive water released from the reaction of DCPD and  $\text{Ca}(\text{OH})_2$  penetrates through the FEP tube ends into the pore space of alumina powder layer, maintaining the appropriate hydrothermal condition inside the capsule I. Thus, the alumina layer serves as an escape space for water as well as a medium for pressure application.

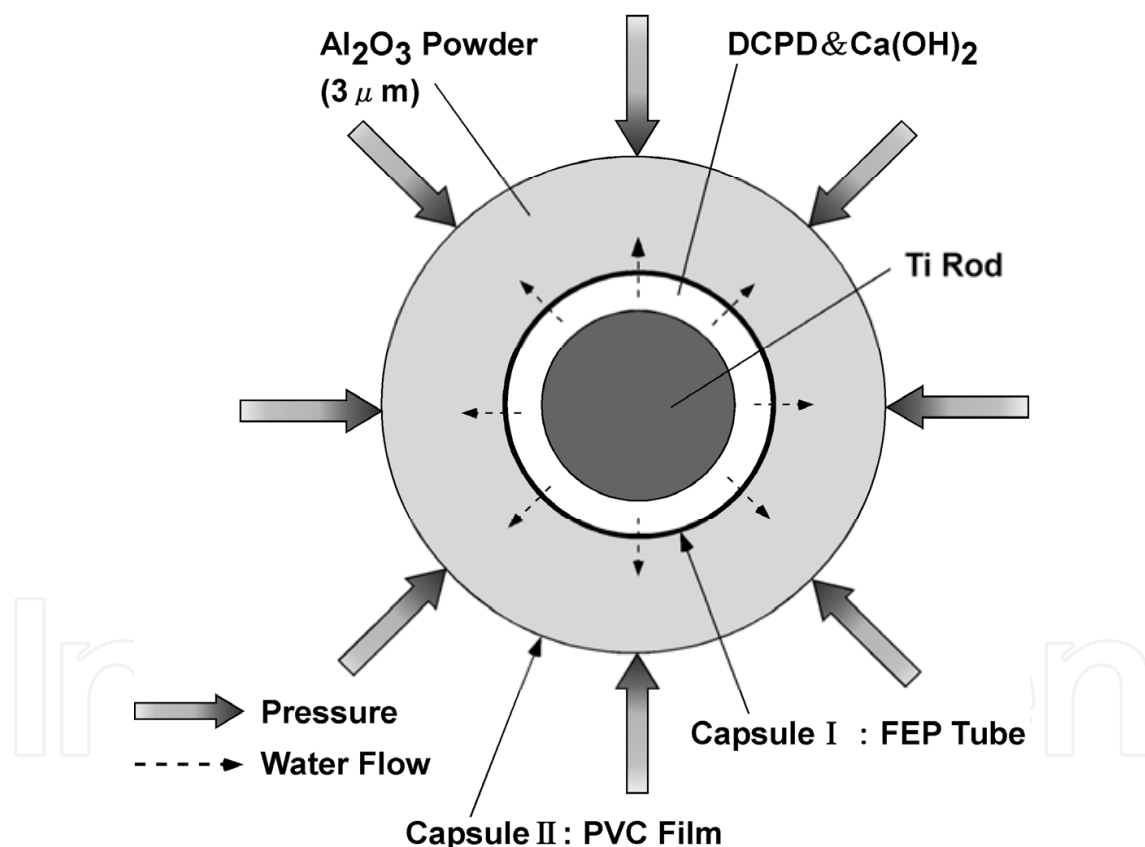


Fig. 11. Schematic illustration of the concept of the double layered capsule hydrothermal hot-pressing (DC-HHP) method.

The capsules prepared were put into a batch type high temperature and pressure vessel (volume: 300ml, SUS316L, AKICO, Japan) for hydrothermal treatment. A schematic illustration of the hydrothermal treatment is shown in Fig.13. The deionized water in the vessel serves as a medium for isostatic pressing (mechanical compaction). The vessel was heated up to 135°C at a heating rate of 5°C/min, and then the temperature was kept

constant. The maximum allowable temperature of the PVC film used for capsule II is 140°C, and the treatment temperature was set to be 135°C due to the temperature limitation. The pressure was kept at 40MPa using pressure regulator. After the treatment, the vessel was naturally cooled down to a room temperature, and the capsules removed from the vessel. In order to investigate the effects of treatment time on the HA coating properties, the treatment time was varied within the range of 3-24 hours.

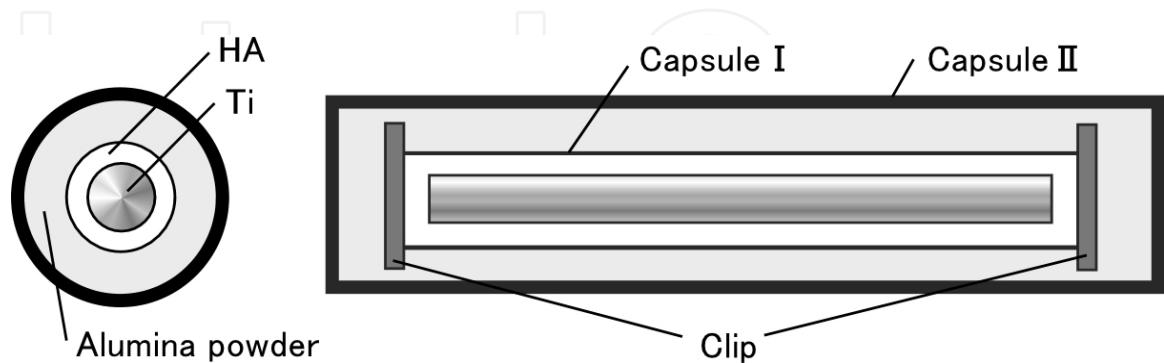


Fig. 12. Schematic illustrations of a double layered capsule in a cross section view.

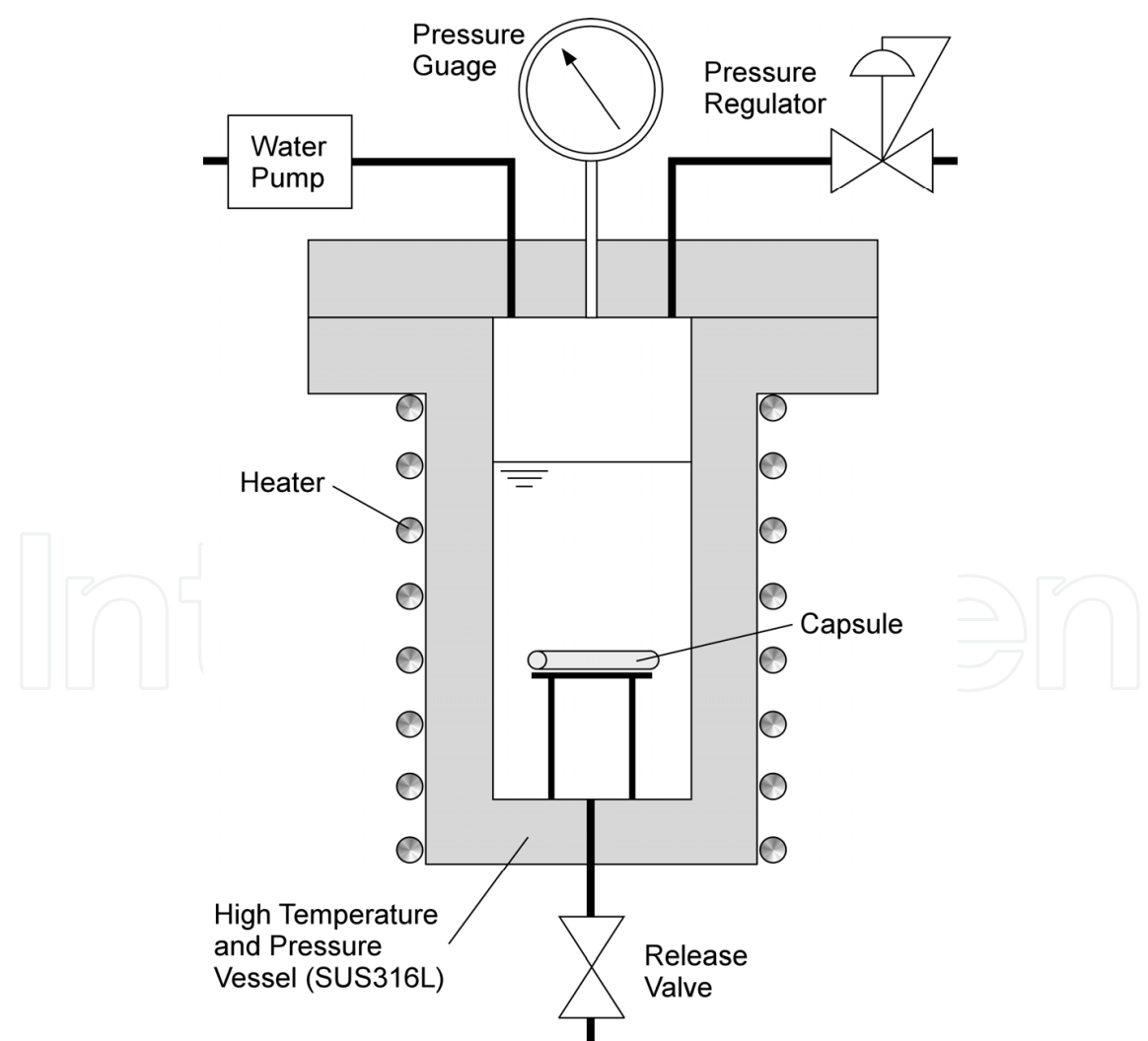


Fig. 13. Schematic illustration of the hydrothermal method and the capsule used in this study.

### 4.3 Adhesion properties evaluation

Pull-out tests were conducted in order to evaluate the adhesion strength of the HA ceramics coating. A schematic illustration of the pull-out testing method used is drawn in Fig.14. The HA coated samples were embedded into an epoxy resin (Sumitomo 3M, Japan) placed in a sample attachment. According to the supplier, the tensile and shear strength of the epoxy resin used were measured to be approximately 29.4 and 11.8 MPa, respectively. And then the protruding part of the HA coating was removed with a grinder and a knife. In order to identify the crystals in the treated specimens, the removed HA coating material was applied to power X-ray diffraction analysis (XRD; MX21, Mac Science, Japan) with  $\text{CuK}\alpha$  radiation 40kV 40mA at a scanning speed of  $3.00^\circ/\text{min}$  with a scanning range ( $2\theta$ ) from  $10^\circ$  to  $40^\circ$ . The microstructure of the coating surface was observed by scanning electron microscopy (SEM; S4300, Hitachi, Japan).

The specimens were loaded with an Instron-type testing machine at a cross-head speed of 0.5mm/min until the Ti rods were pulled out entirely. The sample attachment was connected to a universal joint. The upper part of the Ti rod was gripped with a manual wedge grip and then loaded with the testing machine through a load-cell. The load  $P$  and cross-head displacement  $\delta$  were recorded during the tests. In order to evaluate the adhesion properties of the HA coating on Ti rod quantitatively, the shear strength and fracture energy were calculated from the results of the pull-out testing. The shear fracture strength,  $\tau$  is computed using the following equation:

$$\tau = \frac{P}{\pi dL} \quad (3)$$

where  $d$  is the diameter of Ti rods(1.5mm),  $L$  is the embedment length of Ti rods,  $P$  is the load. The fracture energy,  $G$  is calculated using the following equation:

$$G = \frac{A}{\pi dL} \quad \left( A = \int_0^{\delta_c} P d\delta \right) \quad (4)$$

where  $\delta$  is the cross-head displacement and  $A$  is the area under the load versus cross-head displacement up to the complete pull out displacement,  $\delta_c$ .

### 4.4 Results and discussion

As demonstrated in Fig.15, HA ceramic layers could be coated to the all surface of Ti rods at the low temperature of  $135^\circ\text{C}$  using the above-mentioned DC-HHP method. The thickness of the HA coating layers could be controlled by the volume of the HA starting powder placed in capsule I, and the thickness range achieved in this study was  $10\ \mu\text{m}$ –1 mm. The experimental results for the thickness of  $50\ \mu\text{m}$  will be presented below. When the seal tightness of capsules II was imperfect, the water placed in the vessel was observed to penetrate into the inner space of the capsules and the HA coating could not be achieved. It was critically important that the inner space of the capsules was vacuumed prior to the hydrothermal treatment in order to check and ensure the seal tightness of the capsules.

XRD profiles of the HA coating layers are shown in Fig.16 for the different treatment times. Only the peaks for HA are observed for the treatment time of 12 and 24 hours, whereas the HA layer prepared with the treatment time of 3 and 6 hours includes the phases of the starting materials or the precursors. Thus, it is understood that the treatment time longer

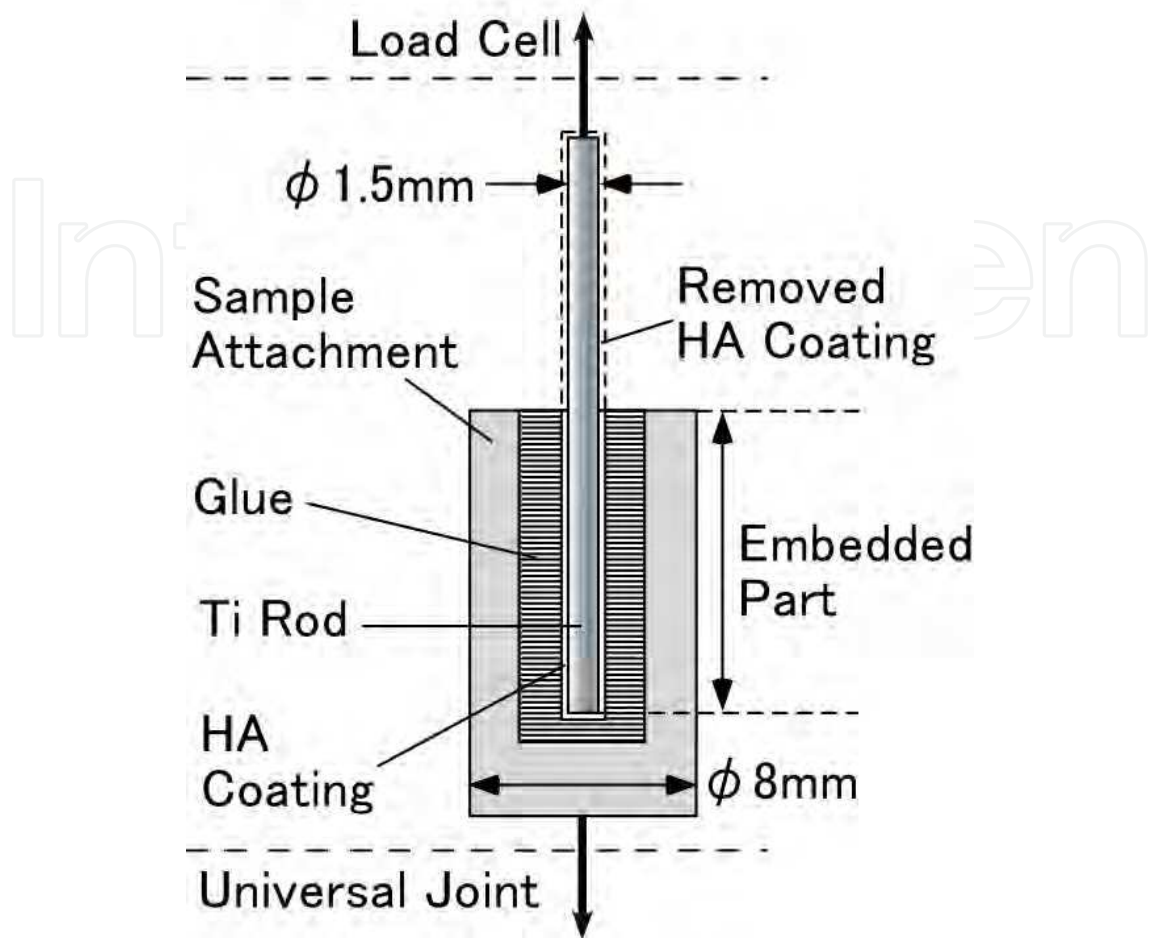


Fig. 14. Schematic illustration of the pull-out testing method in a cross section view.

than 12 hours was required to convert the starting powders to HA entirely. The crystallinity of the HA coating is observed to increase with the increasing treatment time, as indicated by the intensity of the peaks. Furthermore, the XRD analysis shows that the low temperature hydrothermal method induced no chemical decomposition unlike high temperature methods such as a plasma spraying method.

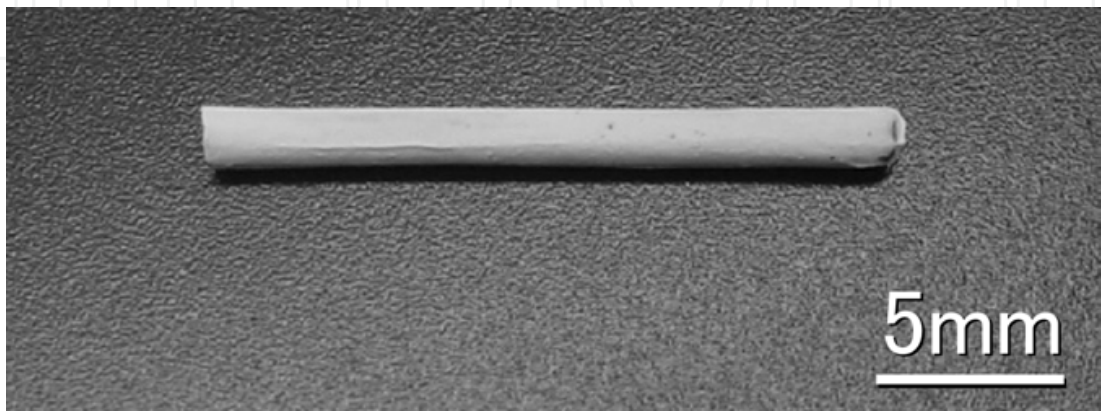


Fig. 15. Photograph of the sample of HA ceramic coating on Ti rod.

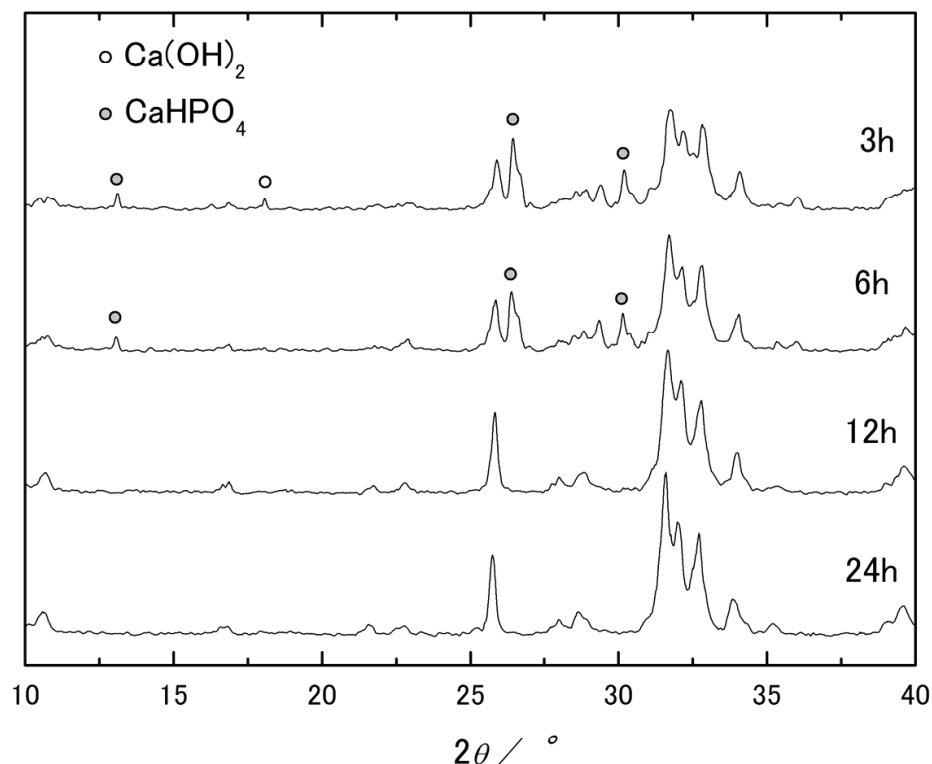


Fig. 16. XRD profiles of the HA coatings treated for 3,6,12 and 24hours, respectively.

The load-displacement curves obtained from the pull-out tests are shown for the treatment time of 24 hours in Fig.17. Fig.18 shows the appearance of the specimen after the pull-out testing for the treatment time of 24 hours. The right-hand side of the specimen show the region where the HA coating was completely stripped off from the Ti rod before the pull-out test. The white part of the specimen (the left-hand side) was initially embedded in the epoxy resin and corresponds to the region that was pulled out after the test. It is clearly seen that the surface of the embedded Ti rod (the left-hand side) is completely covered with the remaining HA layer. An SEM micrograph of the pull-out part in Fig.18(a) is given in Fig.18(b). The appearance of the scratched surface indicates that significant abrasion of the HA layer took place in the pull-out process. It is demonstrated from Fig.18(a) that the crack propagation took place not along the HA/Ti interface, but in the HA coating layer. The crack path was always located within the HA coating irrespective of the different treatment times. This observation suggests that the fracture toughness of the HA/Ti interface is close to or higher than that of the HA ceramics only. If the interface between the HA and Ti rod was held just by interfacial friction with no significant chemical bond, no HA ceramics would remain on the Ti rods after the pull-out testing.

In all the load-displacement curves, there is observed so-called pop-in behavior where the load sharply decreases at the load level indicated by arrow and then increases again until the peak load is reached. The pop-in behavior is considered to correspond to the onset of the crack propagation. The load ascending part after the pop-in may suggest that the initiated crack deviated from its original crack orientation and propagated into the HA coating away from the HA/Ti interface region. The deviation of the crack path from the HA/Ti interface region may induce an additional frictional resistance to the crack propagation in the pull-out process. Indeed, significant abrasion of the HA coating layers was observed on the fracture surface after the pull-out tests, as shown in Fig.18(a).

The post-peak of the load-displacement curves is characterized by the load descending part due to a stable pull-out process of the Ti rod. It is seen that the critical displacement at which the applied load become zero is close to the embedded length of the Ti rod (approximately 10 mm).

In order to evaluate quantitatively the bonding characteristics of the HA coatings, the shear strength and fracture energy were calculated from the load-displacement curves of the pull-out tests. Two shear strength parameters were calculated in this study. Hereafter, the shear strength parameters computed from the pop-in load, and the peak load are designated by  $\tau_i$  and  $\tau_{max}$ , respectively. The calculated shear strength of each surface modifying conditions in Table.3 are plotted in Fig.19 as a function of the treatment time. The data of  $\tau_{max}$  shown in Fig.19 are the averaged results obtained from at least 4 specimens.

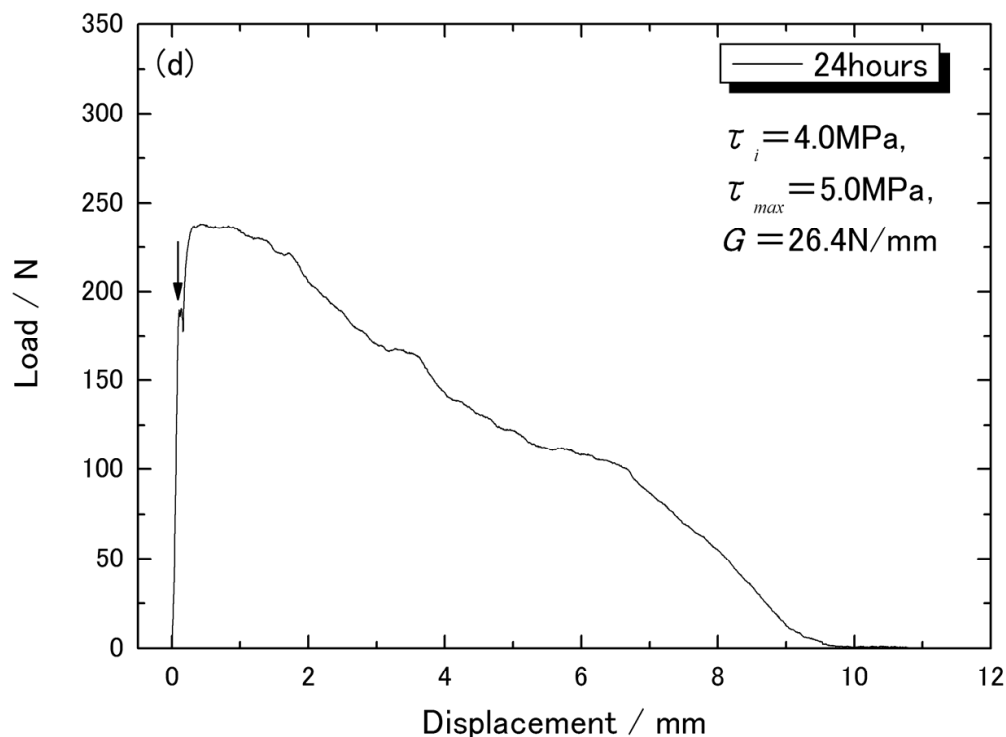


Fig. 17. Load-Displacement curve of the pull-out testing for the HA coatings treated for 24 hours.



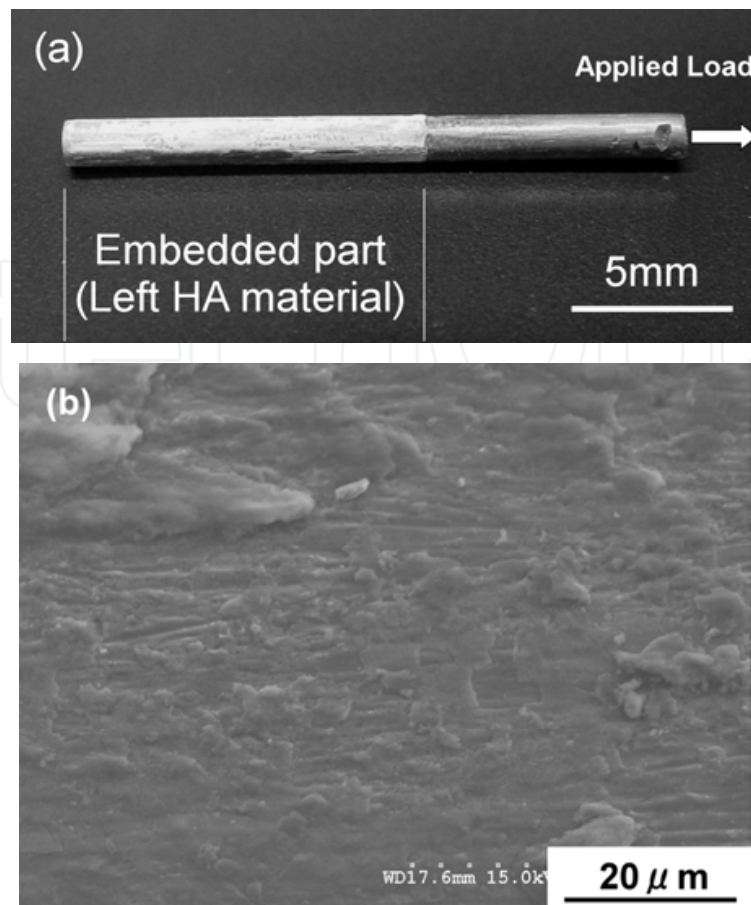


Fig. 18. Photograph of the specimen after pull-out testing (treated for 24hours) and SEM micrograph.

It is seen that the  $\tau_i$  gives an almost constant value (4.1 to 4.6 MPa) irrespective of the treatment time, even though there is a slight increase in the  $\tau_i$  for the treatment time of 6 and 12 hours. The  $\tau_{max}$  initially increased and then gradually decreased when the treatment time was longer than 6 hours. The “HYDRO” specimens showed the highest strength in the DC-HHP as well as the HHP processing. It has been shown in our recent experiment that the adhesion of the HA ceramics bonded on Ti using the conventional HHP method decreased also for longer treatment times [Onoki et al, 2003b]. It should be remembered that treatment time longer than 12 hours was needed for the complete conversion of the starting materials into pure HA, and some starting materials remained in the solidified layers for the shorter treatment times. The above-mentioned experimental results suggest that there may be an optimal hydrothermal treatment time for the production of pure and stronger HA coatings. The adhesion properties measurements and XRD analyses indicates that the treatment time of 12 hours is the suitable condition for the HA coating by DC-HHP method under 135 °C and 40 MPa. Our approximate estimates using the Archimedes’ method have shown that the density of the HA coating initially increased until the treatment time of 6 hours and then gave a constant value for the longer treatment time (the measured density was 1.6 g/cm<sup>3</sup> for 3hours, and 1.9g/cm<sup>3</sup> for the longer treatment time). Thus, the initial increase in the adhesion properties may be due to the formation of HA and its densification. The XRD profiles in Fig.16 suggests that the crystal size of the HA for the treatment time of 12 hours may be larger than that for 24 hours. This observation may provide a possible explanation for the decreased adhesion properties for the

longer treatment time. However, more detailed examination is needed in order to discuss the reason for the presence of such an optimal treatment time. Now investigation of the bonding mechanism in the HHP process is now in progress.

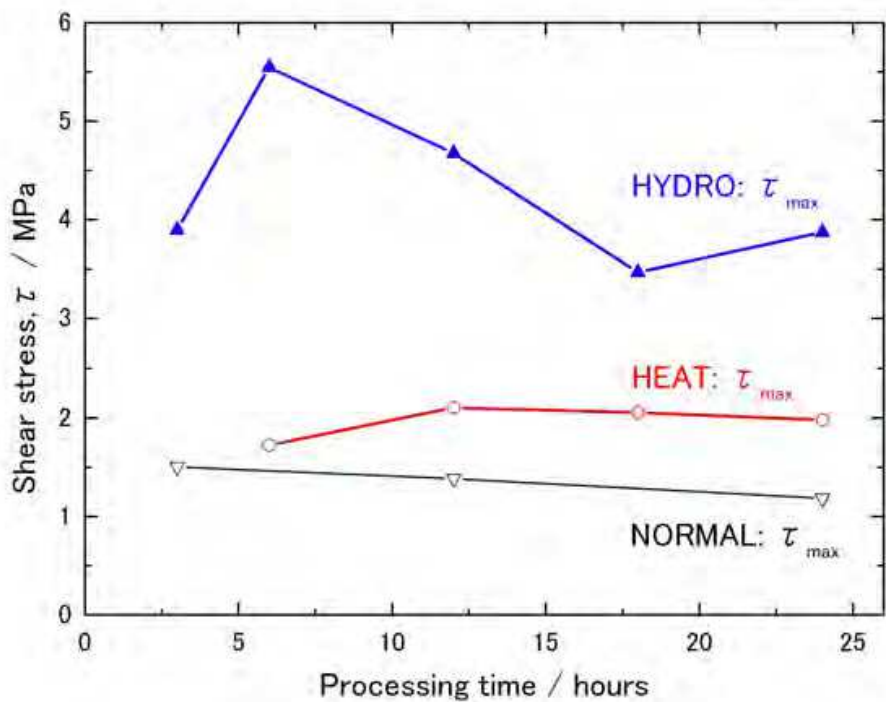


Fig. 19. Relationship between HA coating adherence and hydrothermal treatment time.

5. Micro structure of HA ceramics by HHP method

SEM photograph of the detached HA layer surface is shown in Fig.20. As exemplified in the figure, the microstructure of the HA layers prepared in this study is composed of the number of pores. The maximum dimension of the pores was observed to be approximately 20  $\mu\text{m}$ . The microstructure of the HA layers prepared with the different treatment times was similar to the one shown in Fig.20. The density of the HA layers as determined by the Archimedes method was approximately 1.9  $\text{g}/\text{cm}^3$ , regardless of the different treatment times. The relative density was calculated to be approximately 60 %, assuming the theoretical density of HA (3.16  $\text{g}/\text{cm}^3$ ). HA ceramics have been also synthesized using the conventional hydrothermal hot-pressing (HHP) method in our previous section, where a uniaxial load was applied to the starting powers using upper and lower loading rods in order to produce high pressure environments. The density of the HA ceramics prepared by the conventional HHP method has been measured to be approximately 1.9  $\text{g}/\text{cm}^3$ , when the treatment temperature and pressure were the same as the conditions used in this study. The agreement in the density suggests that it may be possible to produce suitable hydrothermal conditions employing the HHP and the DC-HHP method developed in this study. It is seen that the density of the HA layers prepared falls in the range of those for human bone (1.6-2.1  $\text{g}/\text{cm}^3$ ). Therefore, it may be possible to adjust and tailor the elastic modulus of HA coatings using the DC-HHP method and to mitigate the stress shielding due to the misfit in the elastic modulus [Hench, 1998]. The above-mentioned physical properties and the porous microstructure of the HA ceramic coatings prepared by the DC-HHP method may be

beneficial to enhance the osteoconductivity and osteointegrativity of orthopedic and dental implant materials in comparison with dense HA ceramic coatings. It was confirmed that pigmented ink fully penetrated the HA ceramics made by the HHP, and that the HA ceramics had open pore structure.

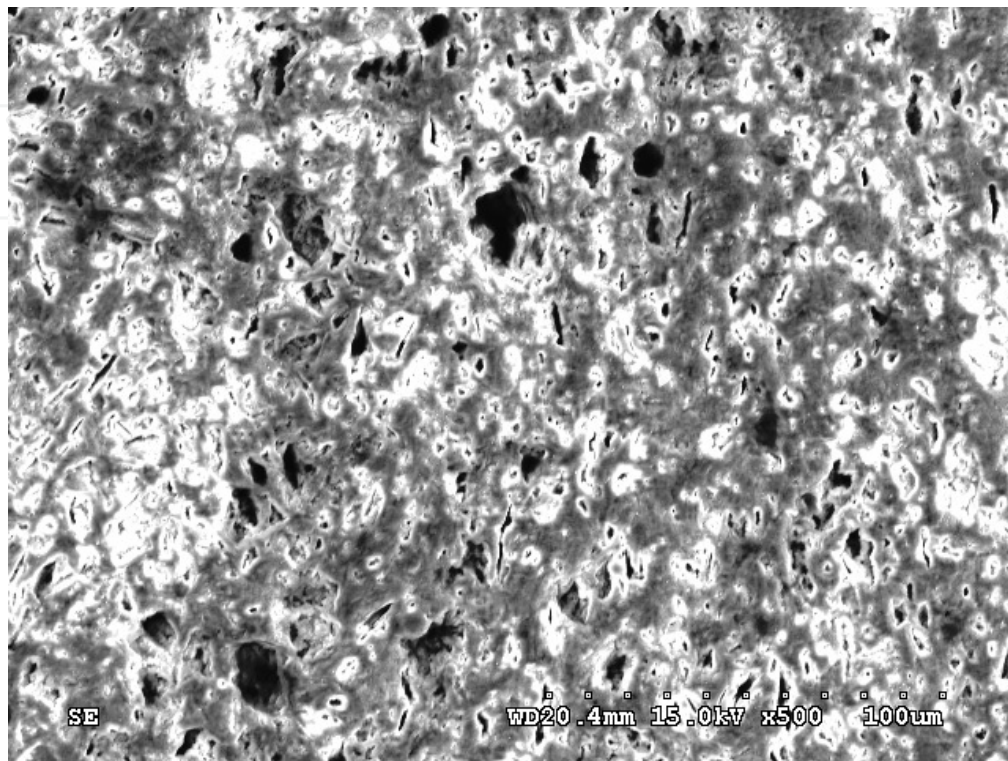


Fig. 20. SEM Photograph of the HA surface produced by the HHP method.

## 6. Conclusions

In this chapter, Ti surfaces were characterized with X-ray photoelectron spectroscopy (XPS) in order to explain the mechanism of bonding Ti and hydroxyapatite (HA) ceramics by hydrothermal hot-pressing (HHP). XPS characterization revealed differences in the Ti surfaces properties between water and air in finishing circumstances. Compared with the air finishing Ti samples, the O 1s region XPS spectra of the water finishing Ti samples was significantly assigned hydroxide or hydroxyl groups (OH<sup>-</sup>) and hydrate and/or adsorbed water (H<sub>2</sub>O). It was clarified that Ti surfaces finished in only water environment could achieve the bonding to HA ceramics.

Secondly, it was investigated how Ti surface modifications affect the interface fracture toughness in HA/Ti bodies prepared by the hydrothermal hot-pressing method. It was revealed that hydrothermal treatment technique, in which the Ti specimen was exposed to 5M NaOH at 423 K for 2 hours, was most effective. The hydrothermal method provided the highest interface fracture toughness (0.35 MPam<sup>1/2</sup>) among the Ti surface modification methods used in this study, while the interface fracture toughness for the other two methods was slightly lower than that obtained for the specimen with no Ti surface modification (0.25 MPam<sup>1/2</sup>). The enhancement of the interface fracture toughness for the hydrothermal surface modification was probably due to the presence of anatase formed on the Ti surface and the good adhesion in the reaction layer. It was shown that the first

successful attempt to form direct bonding between the Ti-based bulk metallic glass:  $\text{Ti}_{40}\text{Zr}_{10}\text{Cu}_{36}\text{Pd}_{14}$  and HA bulk ceramics. The bonding could be obtained in only cases of the BMG with the GIL. It was demonstrated that a series of hydrothermal techniques could be very useful for bonding bulk ceramics and bulk metallic materials. The surface of the Ti-based BMG can be made bioactive by coating bioactive ceramics like as hydroxyapatite (HA) through the low temperature techniques in the range of RT and 150°C. In order to form a growing integrated layer (GIL) on the BMG surface for improving adhesive properties to HA ceramics, the BMG substrates needs to be treated in 5mol/L NaOH solution at 90°C for 120 minutes by hydrothermal-electrochemical techniques. Hydrothermal hot-pressing (HHP) treatment (150°C, 40MPa, 2hours) of the BMG and powder mixture of  $\text{CaHPO}_4 \cdot 2\text{H}_2\text{O}$  and  $\text{Ca}(\text{OH})_2$  is appropriate way for bonding the BMG and HA ceramics because of low operating temperature.

Additionally, it was demonstrated that HA ceramics could be coated to Ti rods at the temperature as low as 135°C by using the newly developed double capsule HHP method (DC-HHP method). Thickness of the HA coating prepared was approximately 50µm. No chemical decomposition and no impurity was observed in the XRD analyses of the HA coating prepared by DC-HHP method. The HA coating layer was shown to have a porous microstructure with the density of 1.9 Mgm<sup>-3</sup> and the relative density of approximately 60 %, which is relatively close to those of human bone. In order to evaluate the adhesion properties of the HA coatings on the Ti rods, pull-out tests were conducted. It was revealed that the crack propagated not along the HA/Ti interface but within the HA ceramic layer in the pull-out tests. The fracture property of the HA/Ti interface was suggested to be close to or higher than that of the HA ceramics. The shear strength obtained from the pull-out tests was in the range of 4.0-5.5 MPa. Finally, it was demonstrated that various hydrothermal techniques were very useful and effective to hydroxyapatite ceramics coating on various Ti metallic materials.

## 7. Acknowledgment

These works were partly supported by “Grant-in-Aid for Cooperative Research Project of Nationwide Joint-Use Research Institutes on Development Base of Joining Technology for New Metallic Glasses and Inorganic Materials” and “Grant-in-Aid for Young Scientists (B), 18760516” from the Ministry of Education, Science, Sports, and Culture of Japan.

## 8. References

- Aoki, H. (1994). *Medical Applications of Hydroxyapatite*, Ishiyaku Euro-America, ISBN1-56386-023-6, Tokyo.
- Asami, K. & Hashimoto, K. (1977). The X-ray photo-electron spectra of several oxides of iron and chromium. *Corrosion Sci.*, 17, 559-570.
- Ashby, M. F. & Greer, A. L. (2006). Metallic glasses as structural materials. *Scripta. Mater.*, 53, 321-326.
- Bavykin, D. V., Friedrich, J. M. & Walsh, F. C. (2006). Protonated titanates and  $\text{TiO}_2$  nanostructured materials: synthesis, properties, and applications. *Adv. Mater.*, 18, 2807-2824.
- Beck, T. R. (1973). Electrochemistry of freshly-generated titanium surfaces I. Scraped-rotating-disk experiments. *Electrochem. Acta.*, 18, 807-814.



- Greer, A. L. (1995). Metallic glasses. *Science*, 267, 1947-1953.
- Hench, L. L. (1998). Bioceramics. *J. Am. Ceram. Soc.*, 81, 1705-1733.
- Hanawa, T. & Ota, M. (1992). Characterization of surface film formed on titanium in electrolyte using XPS. *Appl. Surf. Sci.*, 55, 269-276.
- Hashida, T. (1993). Fracture toughness testing of core-based specimens by acoustic emission. *Int. J. Rock Mech. Min. Sci. Geomech. Abstr.*, 30, 61-69.
- Hosoi, K., Hashida, T., Takahashi, H., Yamasaki, N., & Korenaga, T. (1996). New Processing Technique for Hydroxyapatite Ceramics by the Hydrothermal Hot-Pressing Method. *J. Am. Ceram. Soc.*, 79, 2771-2774.
- Inoue, A. (2000). Stabilization of metallic supercooled liquid and bulk amorphous alloys. *Acta Mater.*, 48, 279-306.
- Kaneko, S., Tsuru, K., Hayakawa, S., Takemoto, S., Ohtsuki, C., Ozaki, T., Inoue, H. & Osaka, A. (2001). In vivo evaluation of bone-bonding of titanium metal chemically treated with a hydrogen peroxide solution containing tantalum chloride. *Biomaterials*, 22, 875-881.
- Kelly, E. J. (1982). Electrochemical behavior of titanium. *Mod. Aspect. Electrochem.*, 14, 319-424.
- Kim, H. M., Miyaji, F., Kokubo, T. & Nakamura, T. (1997). Effect of heat treatment on apatite-forming ability of Ti metal induced by alkali treatment. *J. Mater. Sci.: Mater. Med.*, 8, 341-347.
- Kim, H. M., Kokubo, T., Fujibayashi, S., Nishiguchi, S. & Nakamura, T. (2000). Bioactive macroporous titanium surface layer on titanium substrate. *J. Biomed. Mater. Res.*, 52, 553-557.
- Kokubo, T. & Takadama, H. (2006). How useful is SBF in predicting in vivo bone bioactivity? *Biomaterials*, 27, 2907-2915.
- Kokubo, T., Kim, H. M., Kawashita, M. & Nakamura, T. (2004). Bioactive metal: preparation and properties. *J. Mater. Sci. Mater. Med.*, 15, 99-107.
- Li, B. Y., Rong, L. J. & Li, Y. Y. (2000). Stress-strain behavior of porous Ni-Ti shape memory intermetallics synthesized from powder sintering. *Intermetallics*, 8, 643-646.
- Long, M. & Rack, H. (1998). Titanium alloys in total joint replacement--a materials science perspective. *Biomaterials*, 19, 1621-1639.
- Ohtsuki, C., Iida, H., Hayakawa, S. & Osaka, A. (1997). Bioactivity of titanium treated with hydrogen peroxide solution containing metal chlorides. *J. Biomed. Mater. Res.*, 35, 39-47.
- Onoki, T., Hosoi, K. & Hashida, T. (2003a). JOINING HYDROXYAPATITE CERAMICS AND TITANIUM ALLOYS BY HYDROTHERMAL METHOD. *Key Eng. Mater.*, 240-242, 571-574
- Onoki, T., Tanaka, M., Hosoi, K. & Hashida, T. (2003b) Proceedings of the 15th Symposium on Functionally Graded Materials, ISBN 4-9901902-0-3, Sapporo, Japan, Nov. 20-21 2003, 1-4.
- Onoki, T., Hosoi, K. & Hashida, T., (2005). New Technique for Bonding Hydroxyapatite Ceramics and Titanium by Hydrothermal Hot-pressing Method. *Scr. Mater.*, 52, 767-770.
- Onoki, T. & Hashida, T. (2006). New method for hydroxyapatite coating of titanium by the hydrothermal hot isostatic pressing technique. *Surf. Coat. Tech.*, 200, 6801-6807.
- Onoki, T., Hosoi, K., Hashida, T., Tanabe, Y., Watanabe, T., Yasuda, E. & Yoshimura, M. (2008a). Effects of titanium surface modifications on bonding behavior of

- hydroxyapatite ceramics and titanium via hydrothermal hot- pressing. *Mater. Sci. Eng. C*, 28, 207-212.
- Onoki, T., Wang, X., Zhu, S., Hoshikawa, Y., Sugiyama, N., Akao, M., Yasuda, E., Yoshimura, M. & Inoue, A. (2008b). Bioactivity of Titanium-based Bulk Metallic Glass Surfaces via Hydrothermal Hot-pressing Treatment. *J. Ceram. Soc. Japan*, 116, 115-117.
- Onoki, T., Wang, X., Zhu, S., Sugiyama, N., Hoshikawa, Y., Akao, M., Matsushita, N., Nakahira, A., Yasuda, E., Yoshimura, M. & Inoue, A. (2009a). Effects of growing integrated layer [GIL] formation on bonding behavior between hydroxyapatite ceramics and Ti-based bulk metallic glasses via hydrothermal techniques. *Mater. Sci. Eng. B*, 161, 27-30.
- Onoki, T., Higashi, T., Wang, X., Zhu, S., Sugiyama, N., Hoshikawa, Y., Akao, M., Matsushita, N., Nakahira, A., Yasuda, E., Yoshimura, M. & Inoue, A. (2009b). Interface structure between Ti-based bulk metallic glasses and hydroxyapatite ceramics jointed by hydrothermal techniques. *Mater. Trans.*, 50, 1308-1312.
- Onoki, T. & Nakahira, A. (2010a). Effects of titanium polishing environments on bonding behavior of hydroxyapatite ceramics and titanium by hydrothermal hot-pressing. *Mater. Sci. Eng. B*, 173, 72-75.
- Onoki, T., Kuno, T., Nakahira, A. & Hashida, T., (2010b). Effects of titanium surface treatment on adhesive properties of hydroxyapatite ceramics coating by double layered capsule hydrothermal hot-pressing. *J. Ceram. Soc. Japan*, 118, 530-534.
- Onoki, T. & Yamamoto, S. (2010c). Hydroxyapatite ceramics coating on magnesium alloy via a double layered capsule hydrothermal hot-pressing. *J. Ceram. Soc. Japan*, 118, 749-752.
- Onoki, T., Yamamoto, S., Onodera, H. & Nakahira, A. (2011). New technique for bonding hydroxyapatite ceramics and magnesium alloy by hydrothermal hot-pressing method. *Mater. Sci. Eng. C*, 31, 499-502.
- Oswald, M., Hessel, V. & Riedel, R. (1999). Formation of ultra-thin ceramic TiO<sub>2</sub> films by the Langmuir-Blodgett technique - a two-dimensional sol-gel process at the air-water interface. *Thin Solid Films*, 339, 283-289.
- Rohanizadeh, R., Al-Sadeq, M. & LeGeros, R.Z. (2004). Preparation of different forms of titanium oxide on titanium surface: Effects on apatite deposition. *J. Biomed. Mater. Res.*, 71A, 343-352.
- Takadama, H., Kim, H. M., Kokubo, T. & Nakamura, T. (2001). An X-ray photoelectron spectroscopy study of the process of apatite formation on bioactive titanium metal. *J. Biomed. Mater. Res.*, 55, 185-193.
- Wen, H. B., De Wijn, J. R., Cui, F.Z. & De Groot, K. (1998a). Preparation of bioactive Ti6Al4V surfaces by a simple method. *Biomaterials*, 19, 215-221.
- Wen, H.B., Van den Brink, J., De Wijn, J.R., Cui, F.Z. & De Groot, K. (1998b). Crystal growth of calcium phosphate on chemically treated titanium. *J. Cryst. Growth*, 186, 616-623.
- Wei, M., Kim, H.M., Kokubo, T. & Evans, J.H. (2002a). Optimising the bioactivity of alkaline-treated titanium alloy. *Mater. Sci. Eng. C*, 20, 125-134.
- Wei, M., Uchida, M., Kim, H. M., Kokubo, T. & Nakamura, T. (2002b). Apatite-forming ability of CaO-containing titania. *Biomaterials*, 23, 167-172.
- Yamasaki, N., Yanagisawa, K., Nishioka, M. & Kanahara, S. (1986). hydrothermal hot-pressing method: apparatus and application. *J. Mater. Sci. Lett.*, 5, 355-356



- Yang, B. C., Weng, J., Li, X. D. & Zhang, X. D. (1999). The order of calcium and phosphate ion deposition on chemically treated titanium surfaces soaked in aqueous solution. *J. Biomed. Mater. Res.* 47, 213-219.
- Yoshimura, M., Onoki, T., Fukuhara, M., Wang, X., Nakata, K. & Kuroda, T. (2008). Formation of Grown Integrated Layer [GIL] between Ceramics and Metallic Materials for Improved Adhesion Performance. *Mater. Sci. Eng. B*, 148, 2-6.
- Zhu, S. L., Wang, X. M., Qin, F. X. & Inoue, A. (2007). A new Ti-based bulk glassy alloy with potential for biomedical application. *Mater. Sci. Eng. A*, 459, 233-237.



## **Biomaterials Science and Engineering**

Edited by Prof. Rosario Pignatello

ISBN 978-953-307-609-6

Hard cover, 456 pages

**Publisher** InTech

**Published online** 15, September, 2011

**Published in print edition** September, 2011

These contribution books collect reviews and original articles from eminent experts working in the interdisciplinary arena of biomaterial development and use. From their direct and recent experience, the readers can achieve a wide vision on the new and ongoing potentials of different synthetic and engineered biomaterials. Contributions were not selected based on a direct market or clinical interest, than on results coming from very fundamental studies which have been mainly gathered for this book. This fact will also allow to gain a more general view of what and how the various biomaterials can do and work for, along with the methodologies necessary to design, develop and characterize them, without the restrictions necessarily imposed by industrial or profit concerns. The book collects 22 chapters related to recent researches on new materials, particularly dealing with their potential and different applications in biomedicine and clinics: from tissue engineering to polymeric scaffolds, from bone mimetic products to prostheses, up to strategies to manage their interaction with living cells.

### **How to reference**

In order to correctly reference this scholarly work, feel free to copy and paste the following:

Takamasa Onoki (2011). Porous Apatite Coating on Various Titanium Metallic Materials via Low Temperature Processing, Biomaterials Science and Engineering, Prof. Rosario Pignatello (Ed.), ISBN: 978-953-307-609-6, InTech, Available from: <http://www.intechopen.com/books/biomaterials-science-and-engineering/porous-apatite-coating-on-various-titanium-metallic-materials-via-low-temperature-processing>

**INTECH**  
open science | open minds

### **InTech Europe**

University Campus STeP Ri  
Slavka Krautzeka 83/A  
51000 Rijeka, Croatia  
Phone: +385 (51) 770 447  
Fax: +385 (51) 686 166  
[www.intechopen.com](http://www.intechopen.com)

### **InTech China**

Unit 405, Office Block, Hotel Equatorial Shanghai  
No.65, Yan An Road (West), Shanghai, 200040, China  
中国上海市延安西路65号上海国际贵都大饭店办公楼405单元  
Phone: +86-21-62489820  
Fax: +86-21-62489821

© 2011 The Author(s). Licensee IntechOpen. This chapter is distributed under the terms of the [Creative Commons Attribution-NonCommercial-ShareAlike-3.0 License](https://creativecommons.org/licenses/by-nc-sa/3.0/), which permits use, distribution and reproduction for non-commercial purposes, provided the original is properly cited and derivative works building on this content are distributed under the same license.

IntechOpen

IntechOpen